

**EVALUATION OF THE COCHLEAR MICROPHONIC FOR THE DIAGNOSIS OF
NOISE-INDUCED COCHLEAR SYNAPTOPATHY**

by

Natalie Tran

B.Sc., McMaster University, 2018

A THESIS SUBMITTED IN PARTIAL FULFILLMENT OF
THE REQUIREMENTS FOR THE DEGREE OF

MASTER OF SCIENCE

in

THE FACULTY OF GRADUATE AND POSTDOCTORAL STUDIES

(Audiology and Speech Sciences)

THE UNIVERSITY OF BRITISH COLUMBIA

(Vancouver)

June 2021

© Natalie Tran, 2021

The following individuals certify that they have read, and recommend to the Faculty of Graduate and Postdoctoral Studies for acceptance, the thesis entitled:

Evaluation of the Cochlear Microphonic for the Diagnosis of Noise-Induced Cochlear Synaptopathy

submitted by Natalie Tran in partial fulfillment of the requirements for

the degree of Master of Science

in Audiology and Speech Sciences

Examining Committee:

Dr. Anthony T. Herdman, Associate Professor, Audiology and Speech Sciences, UBC

Supervisor

Dr. Navid Shahnaz, Associate Professor, Audiology and Speech Sciences, UBC

Supervisory Committee Member

Dr. Valter Ciocca, Professor, Audiology and Speech Sciences, UBC

Supervisory Committee Member

Abstract

Purpose: Conventional audiometry, used to detect elevated hearing thresholds, is insensitive to cochlear pathologies involving cochlear synapse degeneration in the absence of hair cell or nerve fiber loss. Patients with this pathology—known as cochlear synaptopathy (CS)—report symptoms such as tinnitus and speech in noise difficulty despite clinically normal hearing thresholds. Current methods for identifying CS in animals require immunohistochemistry, however this invasive technique cannot be translated to clinical diagnostics. The present study aims to evaluate the diagnostic potential of the cochlear microphonic (CM) for noise-induced CS via electrocochleography.

Design: The CM in response to 95 dB nHL broadband clicks was recorded via tympanic membrane electrocochleography. 18 music students ($n = 32$; mean age = 21.7) with normal hearing thresholds (≤ 25 dB, HL 250-8000 Hz) and 19 normal hearing controls ($n = 35$; mean age = 22.5) were recruited for the study. Lifetime noise exposure was obtained using the NESI. A repeated-measures ANOVA was used to analyze the effects of music background and rater on CM/CAP amplitude, CM duration, and CM area under the curve. Correlation tests were performed between NESI scores and liberal or conservative CM power calculations. Inter-rater reliability was tested using a multiple regression design. Inter-class correlation tests were performed on liberal and conservative CM/CAP amplitude and CM duration values.

Results: There were no significant group differences on any of the electrocochleography measures. Lifetime noise exposure scores were not significantly different between groups.

Conclusion: The present study found no evidence that CM/CAP amplitude, CM duration, or CM area under the curve are associated with noise exposure. Results suggest 1) no effect of

CS on the cochlear microphonic, 2) electrocochleography is insensitive to CS, or 3) noise exposure is too low to detect CS. It is possible the effects of noise exposure may be observed in individuals with greater lifetime noise exposure than those recruited for the study. Use of tympanic membrane electrocochleography to assess CS in humans remains inconclusive. Additional research is needed to develop a clinical diagnostic protocol for early cochlear damage that precedes hair cell loss.

Lay Summary

Animal studies have shown that inner ear damage can go undetected via conventional audiometric testing—a phenomenon known as “hidden hearing loss”. Traumatic noise exposure can damage sensory cell connections while maintaining normal hearing sensitivity for sounds in quiet. This “hidden” damage can lead to severe hearing difficulty later in life. In humans with normal hearing sensitivity, it is possible this damage can present as tinnitus, sound sensitivity, or difficulty of speech perception in noise. Instead of using soft sounds in quiet, loud sounds have been proposed to better detect this “hidden” inner ear damage. Current research measuring physiological neural responses to loud noise is inconclusive, highlighting the need for a more sensitive test. This study evaluates the potential for using physiological recordings of inner ear sensory cell electrical activity as a tool for detecting inner ear damage, particularly in the absence of behavioural hearing deficits.

Preface

All of the work presented henceforth was conducted in the Middle Ear Laboratory and BRANE Laboratory at the University of British Columbia, Vancouver campus. This thesis project is part of a larger, ongoing research project on cochlear synaptopathy at the University of British Columbia's Middle Ear Laboratory. This thesis is an original intellectual product by myself, Natalie Tran, with guidance and mentorship from my supervisor Dr. Anthony Herdman, and my professors Dr. Navid Shahnaz and Dr. Valter Ciocca. The study design and data analyses were conceptualized by myself with guidance from Dr. Anthony Herdman, whom provided advice and consultation throughout the duration of this process.

An electrocochleography protocol developed by myself and Dr. Anthony Herdman, along with original data, was intended for this thesis project. However, due to unprecedented research restrictions on campus, the project shifted to a retrospective analysis. Subject data was provided by Charlene Chang from her own thesis project titled “Electrocochleography as a Diagnostic Tool for Noise-Induced Cochlear Synaptopathy”. Participant recruitment and test administration for the larger project were carried out by myself, Charlene Chang, Ainsley Ma, and Stéphanie Monette. All electrocochleography data were collected by Charlene Chang (co-investigator). Data analysis was completed by myself under the guidance of Dr. Anthony Herdman. Dr. Navid Shahnaz assisted in the development of the larger project's creation and execution.

All procedures were approved by the University of British Columbia Clinical Research Ethics Board as part of a larger study, certificate number H16-02052, under the project title “Hidden Hearing Loss - HHL”.

Table of Contents

Abstract	iii
Lay Summary	v
Preface	vi
Table of Contents	vii
List of Tables	xi
List of Figures	xii
List of Abbreviations	xiii
Acknowledgements	xv
Dedication	xvi
Chapter 1: Introduction	1
1.1 Typical Physiology of the Auditory System	2
1.2 Cochlear Synaptopathy (CS)	4
1.2.1 Mechanisms of CS.....	8
1.2.1.1 Possible Implications for the Efferent System.....	11
1.2.2 Similarities to Auditory Neuropathy Spectrum Disorder (ANSD).....	13
1.2.3 Clinical Presentations of CS	15
1.3 Electrophysiological Assessments of CS.....	17
1.3.1 Auditory Brainstem Response Wave I Amplitude	17
1.3.2 Envelope-Following Response	19
1.3.3 Middle Ear Muscle Reflex.....	20

1.3.4	Electrocochleography (ECochG).....	21
1.3.4.1	The Cochlear Microphonic (CM).....	22
1.3.4.1.1	CM Duration and Amplitude in ANSD	23
1.4	Musicians and Noise Exposure.....	25
1.5	Purpose of the Study.....	27
1.6	Hypothesis	28
Chapter 2: Methods.....		29
2.1	Data Source.....	29
2.2	Subject Records	30
2.2.1	Inclusion Criteria	30
2.2.2	Exclusion Criteria.....	31
2.3	Lifetime Noise Exposure History	33
2.4	ECochG Procedure	33
2.5	Waveform Analysis.....	35
2.5.1	CM Duration Measurement	39
2.5.2	CM Amplitude Measurements and CM/CAP Amplitude Ratio	40
2.5.3	CM Power.....	41
2.5.4	Raters	42
2.6	Statistical Analysis.....	43
Chapter 3: Results		44
3.1	Lifetime Noise Exposure History	44
3.2	Electrophysiological Measurements.....	47

3.2.1	CM Duration.....	49
3.2.2	CM/CAP Amplitude Ratio.....	51
3.2.3	CM Power.....	52
Chapter 4: Discussion.....		55
4.1	Summary of Results.....	55
4.1.1	CM Measures.....	55
4.1.1.1	Comparison to Current Literature.....	55
4.1.2	Lifetime Noise Exposure.....	58
4.1.3	Raters.....	58
4.2	Possible Explanations for Current Findings.....	59
4.2.1	ECochG Stimuli and Recording Parameters.....	59
4.2.2	Sensitivity of the CM to CS in Humans.....	63
4.2.3	Effects of Age.....	64
4.2.4	Recruitment and Sample Size.....	66
4.2.5	Noise Exposure and Reliability of NESI.....	67
4.2.6	Human Susceptibility to CS.....	69
4.3	Study Limitations.....	70
4.4	Future Research Directions.....	72
Chapter 5: Conclusion.....		75
Bibliography.....		76
Appendices.....		97
Appendix A	Supporting Documents.....	97

A.1	Pearson's r Correlations	97
A.2	CM ANSD Literature	98
Appendix B	Descriptive Statistics	100
B.1	CM Duration	100
B.3	CM Power	102

List of Tables

Table 2.1 Demographic summary of participants included in analysis	32
Table 3.1 Mean, standard deviation, minimum, and maximum recorded units of noise exposure for high-risk and control groups	45
Table 3.2 Mean, standard deviation, minimum, and maximum recorded units of noise exposure for high-risk and control groups excluding outliers	46
Table 3.3 Pearson correlations ($r(38)$) between NESI and the CM power, CM duration, and CM/CAP amplitude ratio measures for both conservative (con) and liberal (lib) criteria. Bolded values represent significant relationships	47
Table 3.4 Mean and standard deviation of measured values for high-risk and control groups	48

List of Figures

Figure 1.1 Pathway of the lateral and medial efferent feedback loops in response to a sound stimulus.....	4
Figure 1.2 Potential pathophysiological effects of CS on the medial efferent system.....	12
Figure 2.1 Typical waveform averaging on a high-risk participant, obtained from sABR v10.3. Averages are sweeps-weighted, while subtractions are amplitude-weighted.....	38
Figure 2.2 CM power calculated by summing the area under the curve, and dividing by the rater-defined CM latency under liberal or conservative criteria.....	42
Figure 3.1 Scatterplot for all NESI scores between the high-risk musician group and control non-musician group.....	44
Figure 3.2 Scatterplot of NESI scores, excluding outliers, between the high-risk musician group and control non-musician group.....	46
Figure 3.3 Scatterplot of measured CM duration values from three raters between the high-risk musician group and control non-musician group.....	49
Figure 3.4 Scatterplot of calculated measured CM/AP amplitude ratio values from each rater between the high-risk musician group and control non-musician group.....	51
Figure 3.5 Scatterplot of calculated CM power values from each rater between the high-risk musician group and control non-musician group. Measured values under conservative and liberal criteria are shown separately.....	53
Figure 4.1 ECoG recordings from a high-risk participant with possible neural components within subtracted CM-only tracings (RC-CC/2).....	62

List of Abbreviations

ABR - Auditory brain response

ANSD - Auditory neuropathy spectrum disorder

ANF - Auditory nerve fiber

CAP - Compound action potential

CC - Condensation click polarity

CM - Cochlear microphonic

CS - Cochlear synaptopathy

dB - Decibels

dBA - Decibels averaged using “A” weighting

ECochG - Electrocochleography

ET - Extra-tympanic

HL - Hearing level

HHL - Hidden hearing loss

Hz - Hertz

IHC - Inner hair cell

IHS - Intelligent Hearing Systems™

LOC - Lateral olivary complex

LSO - Lateral superior olive

MOC - Medial olivary complex

μV - Microvolts

ms - Milliseconds

nHL - Normalized hearing level

OHC - Outer hair cell

PVCN - Posterior ventral cochlear nucleus

RC - Rarefaction click polarity

TBI - Traumatic brain injury

TT - Trans-tympanic

TTS - Temporary threshold shifts

VNTB - Ventral nucleus of the trapezoid body

Acknowledgements

My deepest gratitude to Dr. Anthony Herdman—my thesis supervisor—for his unending expertise, care, and humour. I would like to thank my supervisory committee—Dr. Valter Ciocca and Dr. Navid Shahnaz—for their knowledge, perspective, and generosity with resources that made this project possible. Special thanks to Heidi Schaefer for her participation as a rater, Ainsley Ma and Stéphanie Monette for their collaboration in the larger project, and to Charlene Chang for her collection of the data used in this thesis.

This research was funded through a Canada Graduate Scholarship – Masters Canadian Institute of Health Research scholarship, and an Internal Seed Grant by the School of Audiology and Speech Sciences to Dr. Valter Ciocca and Dr. Navid Shahnaz.

A very special thanks to my family in Toronto for their unwavering care and encouragement throughout my education. Their support enabled me to accomplish more than I had imagined.

Dedication

To my family—especially my amazing, resilient mother.

Chapter 1: Introduction

Current conventional audiometry evaluates a person's hearing sensitivity to pure tones from 250-8000 Hz in a sound-attenuated room, with hearing loss being measured via elevated hearing thresholds (>20 dB HL) (Katz, 2015). However, this diagnostic measure may miss some individuals with hearing dysfunction. Clinicians encounter cases in which patients report ongoing hearing difficulties—such as degraded speech intelligibility in noise and chronic tinnitus—despite having hearing thresholds to pure tones within normal limits (<20 dB HL) (Henry, Dennis, & Schechter, 2005; Hind et al., 2011; Roberts et al., 2008; Tremblay et al., 2015). This presence of functional deficits in the absence of measurable hearing intensity deterioration is known as “hidden hearing loss” (HHL) (Schaette & McAlpine, 2011). Consequently, this lack of sensitivity in conventional audiometry can be problematic for clinicians in determining the underlying cause of patients' hearing challenges.

The present study is part of a larger ongoing research project to develop an accessible clinical test battery sensitive to a particular HHL, characterized by its pathophysiology. The purpose of the present study is to determine the diagnostic utility of an electrophysiological measure—which records electrical activity at the level of the cochlea—explained in further detail within this chapter. The aim of the larger ongoing research project is to improve standard audiological evaluations such that HHL may no longer be “hidden”. In order to understand how auditory dysfunction may not be detected by current conventional audiometry, the mechanisms of the natural, healthy auditory pathway must first be understood.

1.1 Typical Physiology of the Auditory System

The cochlea consists of around 12,000 outer hair cells (OHCs) that are important for acoustic non-linear amplification, and 3,500 inner hair cells (IHCs) that transduce sound-evoked mechanical motion into receptor potentials for signal transmission. These hair cells are distributed across the tonotopic cochlea, and are mechanically depolarized via the sound-induced displacement of the basilar membrane. While there are three times as many OHCs than IHCs, IHCs synapse with around 95% of afferent auditory nerve fibers (ANFs) (type-I) whereas OHCs are only innervated by the remaining 5% of ANFs (type-II). The axon bundle of peripheral ANFs are known as the cochlear nerve. Each afferent type-I ANF has one peripheral terminal innervating a single IHC, and each IHC is innervated by several type-I ANFs. IHCs excite type-I ANFs via the release of glutamate neurotransmitters into the synaptic cleft where it is taken up by the receptors in the postsynaptic ANF terminal (Fettiplace, 2017). To do this, synaptic ribbon structures—anchored at the basolateral membrane of hair cells—tether glutamate neurotransmitter vesicles close to the active zone of the synaptic cleft to promote vesicular exocytosis and subsequent neurotransmission (Nouvian, Beutner, Parsons, & Moser, 2006; Parsons & Sterling, 2003). Each synapse has one associated presynaptic ribbon. Neurotransmitter release depolarizes the ANF terminals, increasing firing probability and action potential initiation.

Afferent type-I ANFs project to the cochlear nucleus, which trifurcates into various pathways. One such pathway is the medial efferent negative feedback loop for cochlear amplification (Eggermont, 2017a). When ipsilateral IHCs are depolarized, afferent type-I ANFs innervate the posterior ventral cochlear nucleus (PVCN)—which projects primarily to the

contralateral ventral nucleus of the trapezoid body (VNTB) in the contralateral medial olivary complex (MOC), with some ipsilateral MOC projections (*Figure 1.1*). Myelinated acetylcholinergic and GABAergic efferent projections—from primarily the contralateral MOC with some ipsilateral MOC input—directly innervate the ipsilateral basolateral OHC membrane to inhibit OHC activity. The OHC is hyperpolarized by these efferent connections to decrease the probability of mechanically-activated depolarization. OHCs are important for creating active non-linearity in the cochlear system, allowing for increased auditory amplification and dynamic range. This inhibitory pathway aids in the fine-tuning process of sound input by effectively “dampening” the non-linear cochlear system. Without this braking system the sound-induced depolarization of OHCs may actually exaggerate its feed-forward system by amplifying the mechanical action of the basilar membrane, which in turn reactivates the OHCs. This may result in a prolonged oscillation of OHC activation and deactivation. Additionally, inhibition—or dampening—of OHCs may also serve to prevent synaptic IHC structures from acoustic trauma (Maison, Usubuchi, & Liberman, 2013). A second pathway of the negative feedback system is the lateral efferent feedback loop, where IHCs are indirectly inhibited via unmyelinated efferent innervation to the type-I ANFs from the ipsilateral lateral superior olive (LSO) of the lateral olivary complex (LOC) (*Figure 1.1*). This particular inhibitory process serves to prevent IHC depolarization and glutamate release in cochlear regions outside of the stimulus frequency.

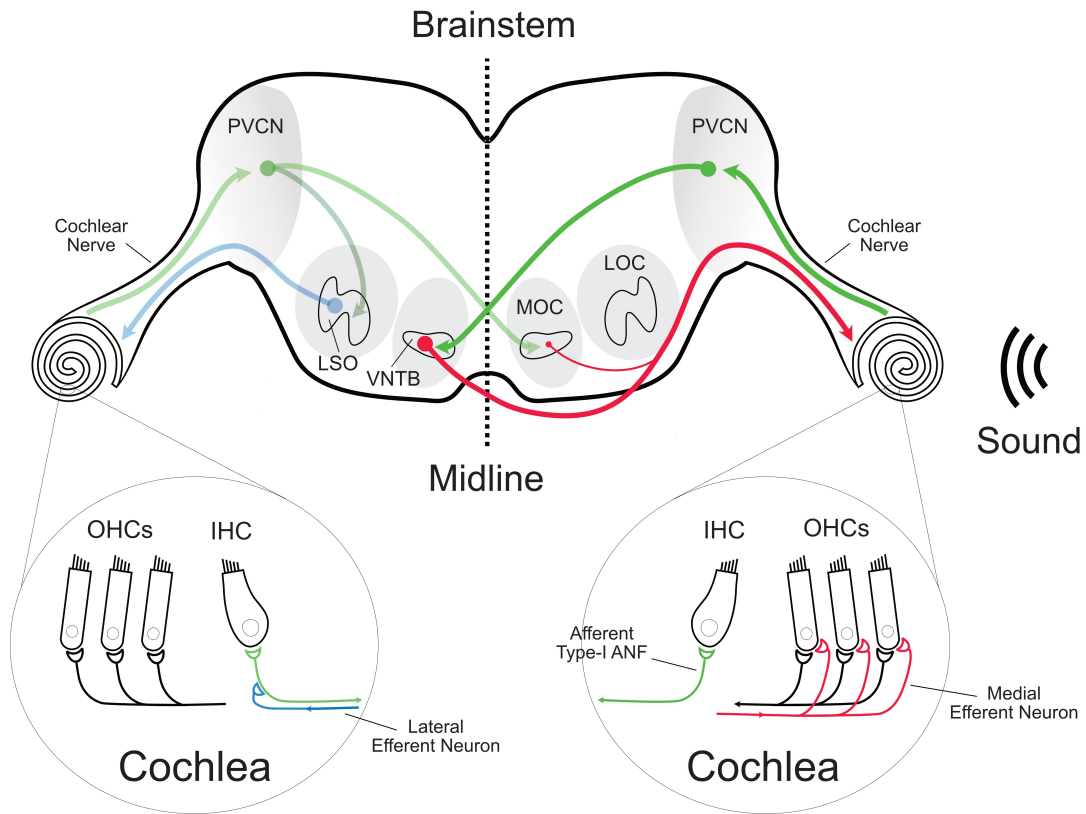


Figure 1.1 Pathway of the lateral and medial efferent feedback loops in response to a sound stimulus. Sound-induced depolarization of the ipsilateral IHC sends afferent excitatory signals to the PVCN via afferent type-I ANFs (green). Faded green arrows show where afferent signals would be sent if IHCs in the opposite cochlea were simultaneously depolarized. PVCN neurons innervate both the ipsilateral LSO of the LOC (faded dark green arrow) and contralateral VNTB of the MOC. Direct, myelinated medial efferent connections represented in red; OHCs ipsilateral to the sound-exposed cochlea are primarily innervated by contralateral MOC connections with some ipsilateral MOC inputs. Indirect, unmyelinated lateral efferent connections represented in faded blue in the opposite cochlea; IHCs in the sound-exposed cochlea are innervated by ipsilateral LSO inputs.

1.2 Cochlear Synaptopathy (CS)

Permanent elevated hearing thresholds are often seen at frequencies where corresponding OHC damage is present (Davis, Ahroon, & Hamernik, 1989). However, several configurations of cochlear damage are often undetected by conventional audiometry (Pienkowski, 2017). One

form of cochlear pathology occurs from synaptic damage between the IHCs and type-I ANFs. Animal studies have shown that conventional behavioural and electrophysiological audiometry is insensitive to partial losses of IHCs or ANFs across the cochlea—that is to say no cochlear “dead regions”—than compared to partial losses of OHCs (Chambers et al., 2016; Liberman et al., 1997; Lobarinas, Salvi, & Ding, 2013; Lobarinas, Salvi, & Ding, 2016). Lobarinas, Salvi, & Ding (2013) showed that in chinchillas with selective carboplatin-induced IHC loss, minimal changes to behavioural audiometric thresholds were seen despite IHC damage exceeding 80%. Interestingly, the same research group found that the pure-tone thresholds were elevated when presented in noise despite an absence of OHC loss (Lobarinas, Salvi, & Ding, 2016). Chambers et al. (2016) reported similar findings, where the deafferentation of over 95% of ANFs in adult ouabain-treated mice—while sparing hair cells—did not elevate behavioural pure-tone thresholds. Sound-evoked neural potentials were also demonstrated to be insensitive to partial hair cell loss (Liberman et al., 1997). These findings indicate that only a small percentage of remaining functional IHC or ANFs are required for the preservation of audiometric pure-tone thresholds, so long as no cochlear “dead regions” or substantial OHC damage are present.

In a seminal study by Kujawa & Liberman (2009), 16 week-old mice were acoustically overexposed to 8-16 kHz noise at 100 dB SPL for two hours. The auditory brainstem response (ABR) was recorded to measure resulting threshold shifts, and otoacoustic emissions (OAEs) measured to assess OHC function. Temporal bones were also harvested at different pre- and post-exposure time periods to observe the effect of noise trauma on the cochlear synapses and cochlear nerve. At 24 hours after noise exposure, tone-pip ABR revealed about a 40 dB threshold shift accompanied with slight OAE elevation. This suggested possible OHC dysfunction with

nerve damage. However, at two weeks post-exposure both ABR thresholds and OAE levels returned to baseline. Immunostaining of harvested temporal bones revealed that, despite reversible (“temporary”) ABR threshold shifts and intact OHCs, roughly 50% of synapses between the IHCs and type-I ANFs were lost just hours after noise exposure while the cochlear nerve showed delayed degeneration only weeks later. No OHC or IHC loss was observed up to one year after noise exposure; their stereocilia remained unaffected. A similar pattern of delayed cochlear nerve degeneration following recovery of threshold shifts and lack of hair cell damage were also demonstrated in guinea pigs (Lin, Furman, Kujawa, & Liberman, 2011). In a subsequent study, they found that exposing mice to varying levels (85-112 dB SPL) and durations (15 minutes to 8 hours) of loud noise resulted in a trend of increasing synaptic loss count with increasing intensity of noise exposure (Fernandez et al., 2020). The observed synaptic losses were an early manifestation of noise injury, except in the higher intensity conditions in which direct OHC damage from noise trauma was observed. Whereas hair cell loss can be seen just hours after noise exposure, ANF loss can be substantially delayed (Kujawa & Liberman, 2006). These studies revealed that noise-induced cochlear synaptic loss can long precede any hair cell loss, and that the pathology would not elevate hearing thresholds on current conventional behavioural and electrophysiological clinical measures. Over time, this pattern of cochlear pathology has become known as cochlear synaptopathy (CS) (Kujawa & Liberman, 2015), and is likely the earliest signs of damage to the auditory system.

Failing to detect CS may have consequences on the future health of the auditory system. Fernandez et al. (2015) investigated age-noise interactions from acute noise overexposure in mice, and found that noise-induced CS could accelerate cochlear aging compared to mice who

were exposed to non-denervating noise levels. However, Sergeyenko, Lall, Liberman, & Kujawa (2013) demonstrated in mice that a loss of ANFs and synaptic ribbons as a function of age, with minimal inner hair cell loss, could occur in the absence of traumatic noise. Similar findings were observed in post-mortem human cochleae where a decrease of around 100 ANFs for every year of life from from birth to 100 years was revealed (Makary et al., 2011; Viana et al., 2015). This age-related cochlear nerve degeneration was proposed by the authors as the basis for human presbycusis and speech in noise difficulty. These studies highlight the importance in identifying early signs of cochlear damage, so that appropriate interventions and prevention methods can be applied to improve patient prognosis.

Current methods for identifying CS in animal models require immunohistochemistry to label remaining cochlear nerve synaptic connections, and involve sectioning of the preserved cochlear system for imaging (Kujawa & Liberman, 2009; Lin, Furman, Kujawa, & Liberman, 2011; Kujawa & Liberman, 2015). However, this invasive technique cannot be translated to human clinical diagnostics, and has only been conducted on post-mortem human organs (Makary et al., 2011; Viana et al., 2015). Electrophysiological and behavioural measures—or a combination of measures within a test battery—have instead been proposed as alternatives to invasive techniques for human clinical diagnosis (Kobel et al., 2017). Several behavioural and electrophysiological measures have since been studied to evaluate their diagnostic potential, although the results have been variable (Bramhall et al., 2019). The development of a human diagnostic tool is important, and requires an understanding of the physiological mechanisms.

1.2.1 Mechanisms of CS

Temporary threshold shifts (TTS) are historically believed to be a protective mechanical process of the acoustic reflex in response to loud noise (Ryan et al., 2016). Instead, Kujawa & Liberman (2009) demonstrated that noise-induced TTS likely occur from the loss of the cochlear synapses between the IHCs and type-I ANFs while the hair cells remain intact. The seemingly temporary shifts were revealed to be a delayed degeneration of the ANF cells that first began with severance from the IHCs. Recovery of threshold shifts back to normal levels was attributed to the return of cochlear function upstream from IHC synapses. Their work highlighted the insufficiency of hearing thresholds as a sole metric for hearing pathology—even when paired with OAEs. Along with hearing threshold monitoring, the researchers investigated possible effects of noise exposure on supra-threshold ABRs. Interestingly, while ABR thresholds and OAE responses in mice appeared to recover to baseline approximately two weeks after exposure, supra-threshold ABR amplitudes showed a sustained decrease in super-high frequencies (32 kHz; an octave band above the 8-16 kHz traumatic noise). This suggested permanent neural loss despite OHC recovery. Considering that the ABR amplitude is influenced by the synchrony of ANFs firing in response to a sound stimulus (Picton, 2010), the amplitude decrease can be attributed to significant loss of IHC-ANF connections. Cochlear synaptic losses can decrease the amount of glutamate being released into the synapse, thus decreasing the firing probability of postsynaptic ANFs (Kujawa & Liberman, 2009; Moser & Starr, 2016). This can result in desynchronized activity among ANFs that manifest as a weakened or delayed ABR waves (Moser & Starr, 2016; Rance & Starr, 2015). This loss may not translate to threshold elevations due to the diffuse nature of synaptic losses and possible involvement of central gain following

deafferentation—a decrease in GABAergic lateral inhibition that compensates for the reduced cochlear output (Salvi et al., 2017).

Importantly, Kujawa & Liberman (2009) revealed the physiological changes in cochlear synaptic loss through the immunostaining of postsynaptic ANF neurofilaments and a presynaptic ribbon structure in order to accurately quantify synaptic losses. Confocal imaging was used to show that the mice exhibited a reduced number of ribbons per IHC and associated terminals 24 hours after noise exposure compared to controls. Unpaired ribbons were found intracellularly away from the basal membrane with signs of swelling. The reduced number of ribbons was prevalent within the octave-band regions above the 8-16 kHz noise stimulus—corresponding to the region of decreased supra-threshold ABR amplitudes—with significantly lower losses in the cochlear region of the octave band and below. While loss of synaptic elements can occur immediately after noise exposure (Kujawa, Suzuki, & Liberman, 2015), a comparable decrease in ANF axon count was only observed 2 years post-exposure. This delayed loss of communication may be due to a loss of neurotrophins normally provided by the hair cells to the ANFs (Glueckert et al., 2008).

The observed pattern of synaptic loss is greater on the modiolar side of IHCs where high-threshold fibers with a lower rate of spontaneous firing are oriented (Liberman, Suzuki, & Liberman, 2015). In quiet, high spontaneous rate, low-threshold ANFs—which activate in response to sounds below 40 dB SPL—are recruited in the presence of a supra-threshold external auditory stimulus (Bharadwaj et al., 2014). Conventional pure-tone audiometry is conducted in quiet, thus only measuring the integrity and synchrony of these low-threshold ANFs. In noisy environments, these low-threshold ANFs become saturated and high-threshold ANFs are then

recruited for sound detection. High-threshold fibers have a wider dynamic range and threshold distribution, and have been suggested as critical fibers for signal coding in background noise (Costalupes, 1985; Young & Barta, 1986). Noise-induced CS selective for high-threshold ANFs is hypothesized to be the cause of HHL (Furman, Kujawa, & Liberman, 2013).

A question that arises from this data is why noise-induced synaptic loss is selective for high-threshold ANF synapses. A possible explanation is that the influx of loud noise produces larger vesicular releases of glutamate, inducing cochlear excitotoxicity and thus a degeneration of nerve terminals (Liberman, 2016). Glutamate is known to have a neurotoxic effect on dendritic terminals when released in large quantities or when poorly recycled back to the presynaptic cell (Pujol & Puel, 1999). The increased vesicular releases of glutamate induce acute swelling of postsynaptic ANF terminals, which then leads to synaptic uncoupling and a loss of function. This pattern of acute synaptic ANF terminal swelling has been shown to occur after exposure to traumatic noise (Wang, Hirose, & Liberman, 2002). Repetitive neurotoxic injury to these terminals can trigger a cascade of metabolic events that eventually results in type-I ANF death (Pujol & Puel, 1999).

It has been proposed that the toxic effect may be more prominent for high-threshold ANFs because 1) the re-uptake of glutamate is less intense on the modular side of the IHC and 2) high-threshold ANFs have fewer mitochondria, which are a source of calcium ion buffering—calcium ions play an important part in the glutamate excitotoxicity cascade (Furman, Kujawa, & Liberman, 2013). High-threshold ANFs also have a lower baseline of neurotransmitter activation, especially since these fibers are not as often recruited in low sound levels compared to low-threshold ANFs that are more often oversaturated at low sound levels. With prolonged exposure

to loud sounds, low-threshold ANFs—that are not as used to large in sustained influxes of glutamate—may become oversaturated as well and be at higher risk of neurotoxicity.

1.2.1.1 Possible Implications for the Efferent System

The depolarization of IHCs—and subsequent afferent signal transmission—activates two negative efferent feedback pathways that provide cochlear protection (see section 1.1). The unmyelinated efferent LOC to type-I ANF circuit hyperpolarizes the afferent peripheral dendrites to prevent excitotoxicity (Pujol & Puel, 2006; Ruel et al., 2001). Disruption to this pathway has been shown to increase vulnerability to acoustic trauma (Darrow, Maison, & Liberman, 2006). Purposeful lesioning of the LOC promoted elevated supra-threshold ABR responses and TTS, while OHCs remained unaffected. A second efferent feedback pathway dampens non-linear OHC activity. OHCs receive direct, myelinated inhibitory efferent inputs from the MOC which hyperpolarize the cell and prevent further depolarization. Without this feedback braking system, OHCs may continually depolarize and repolarize in a positive feed-forward loop due to their active role in adding mechanical energy back into the cochlear partition as they contract in response to the sound input. This feed-forward loop manifests as a sustained, oscillatory “ringing” of hair cell electrochemical activity. Breakdown of this myelinated efferent MOC-OHC pathway via CS may occur if the synaptic loss degrades afferent ANF communication to the cochlear nucleus (*Figure 1.2*).

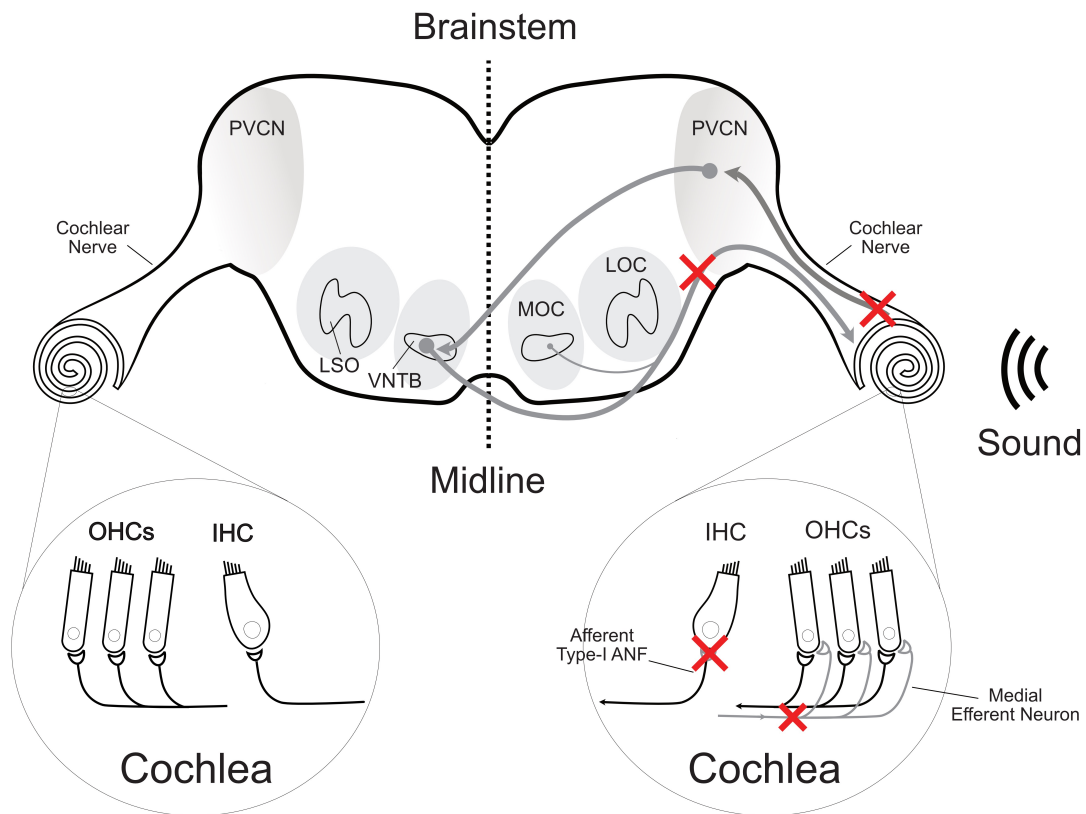


Figure 1.2 Potential pathophysiological effects of CS on the medial efferent system. Loss of IHC synapses may reduce outputs of the PVCN to the MOC, subsequently reducing inhibitory inputs from the MOC to the OHCs and inducing “runaway” feed-forward cochlear amplification. Red x’s represent disruptions to neural communications in the medial efferent circuit.

The MOC-OHC negative feedback system has been proposed to prevent auditory neuropathy via cochlear damping protection (Maison, Usubuchi, & Liberman, 2013). In humans, a dramatic decrease in MOC density is seen in older ears—this loss of MOC feedback may contribute to the age-related decrease in word recognition in noise. (Liberman & Liberman, 2019). Because cochlear fine-tuning is thought to increase dynamic range and speech intelligibility in noise (Lichtenhan, Wilson, Hancock, & Guinan, 2016), disruption of the efferent MOC feedback system may degrade these functional auditory processes. Presently, there is

limited literature about the physiological properties of efferent modulation in response to primary degenerative CS in humans. However, relevant research on other auditory pathologies sharing similar mechanisms to CS may provide some insight.

1.2.2 Similarities to Auditory Neuropathy Spectrum Disorder (ANSD)

Much like CS, a hallmark of auditory neuropathy spectrum disorder (ANSD) is the deterioration of speech intelligibility—particularly in background noise—despite clinically normal hearing thresholds (Star et al., 1996; Zeng et al., 2005). ANSD is clinically defined by normal OHC function via OAEs, and absent or abnormal cochlear nerve responses such as through ABR or the compound action potential (CAP). Another notable characteristic of ANSD is a large and prolonged cochlear microphonic (CM) along with absent or elevated ABRs (Moser & Starr, 2016). The CM is a frequency-following response potential reflecting the depolarization and repolarization of hair cells. Details regarding the CM in cases of ANSD are further discussed in section 1.3.4.1.

As the name implies, ANSD broadly encompasses a spectrum of genetic and acquired pathologies that can be categorized under two classes based on their mechanisms: auditory neuropathy, involving a pathophysiology of the post-synaptic ANFs; or auditory synaptopathy, involving a pathophysiology of the pre-synaptic active zone and its associated synapse (Moser & Starr, 2016). All associated pathologies appear to cause neural dys-synchrony between the cochlea and auditory brainstem (Rance & Starr, 2015). In fact, CS has been proposed as a subclass of ANSD because it shares similar physiological characteristics to pathologies classified under auditory synaptopathy (Moser & Starr, 2016). One example of auditory synaptopathy is

the pathogenetic mutation of the OTOF gene, which codes for the otoferlin protein. Otoferlin is important for IHC vesicular exocytosis (Roux et al., 2006). Its dysfunction can cause an inability to both fuse the vesicle to the hair cell membrane, and replenish glutamate for sustained glutamate release and subsequent neurotransmission (Pangrsic et al., 2010). An example of acquired auditory synaptopathy is hyperbilirubinemia and prolonged neonatal intensive care unit stay in preterm infants (Harrison et al., 2015; Moser & Starr, 2016). Bilirubin ototoxicity is believed to occur at the presynaptic terminals via nitric oxide and calcium ion imbalance (Spencer et al., 2002). Both pathologies degrade IHC-ANF synaptic transmission, and share similarities in functional outcomes with CS (Moser & Starr, 2016).

The disruption of efficient signal transmission leads to neural dys-synchrony, which can manifest in temporal coding deficit (Michalewski et al., 2005). Auditory temporal coding is important for encoding the temporal fine structure of speech; deficits are implicated in speech intelligibility difficulties (Katz, 2015). Temporal coding deficits are also seen in cases of CS (Plack et al., 2014; Song et al., 2016). Like CS, disruption to the efferent negative feedback system, and subsequent “ringing” of the non-linear OHC system, has also been proposed to occur as a result of ANSD (Smith, 2018; Starr et al., 2001). Frequency fine-tuning within the cochlea via OHC modulation is thought to enhance speech intelligibility in noise and the dynamic range of hearing (Lichtenhan, Wilson, Hancock, & Guinan, 2016), both of which have been observed to be deficient in ANSD (Berlin et al., 2010; Vlastarakos et al., 2008). Smith (2018) demonstrated longer CM duration in infants diagnosed with ANSD compared to controls, which indicated prolonged OHC activity in response to sound stimuli. This supports the theory of a disrupted efferent braking system in the presence of ANSD, and further implicates CS as a sub-

class among the spectrum. Because CS can be classified under ANSD based on pathophysiological similarities, evaluation of the diagnostic tools used for ANSD may be promising in the context of noise-induced CS diagnosis.

1.2.3 Clinical Presentations of CS

Currently, there are no gold standard clinical diagnostic measures for CS in humans even though ANF loss accompanied by intact hair cells has been shown to occur in human cadavers (Makary et al., 2011). Viana et al. (2015) observed a decrease of approximately 100 ANFs for every year of life on human postmortem cochleae ranging from new born to 100 years of age—without extensive hair cell damage—suggesting that CS does exist in humans. The authors proposed this pattern of ANF loss to account for the reported speech in noise issues and presbycusis in the aging population. Nonetheless, cases of reported hearing difficulty despite normal audiometric thresholds—otherwise known as “HHL”—can and do show up in the clinic (Plack, Barker, and Prendergast, 2014).

The extent to which CS contributes to hearing difficulties in humans remains unknown. There is documented evidence of patients with a history of noise exposure experiencing tinnitus, speech perception in noise difficulty, and temporal processing deficits despite normal audiometric thresholds (Plack, Barker, & Prendergast, 2014). Approximately 5% of adults and children with normal hearing thresholds experience difficulty understanding speech in noise (Hind et al., 2011), and about 15% of adults report chronic tinnitus in the absence of audiometric threshold shifts (Henry, Dennis, & Schechter, 2005; Roberts et al., 2008). Tinnitus and hyperacusis, with no associated hearing loss, have been proposed to arise from CS as a result of

central gain (Henry et al., 2014; Plack, Barker, & Prendergast, 2014; Schaette & McAlpine, 2011)—where increased neural activity in the auditory cortex and inferior colliculus is thought to be the source (Gu et al., 2010; Salvi et al., 2017). These individuals also exhibit temporal coding deficits (Paul, Bruce, & Roberts, 2017). Particularly, supra-threshold temporal encoding—such as with speech perception in noise—has been measured behaviourally, and is suggested to be reduced by CS (Bharadwaj et al., 2014).

There are several potential etiologies for CS. For example, Cho et al. (2013) exposed mice to compressed air to mimic a head-related blast exposure. While OHC loss was observed in the basal turn of the cochlea, no hair cell loss was observed in the apical end of the cochlea tuned to low frequencies tuning. Despite this, a significant loss of afferent synapses and ANFs was observed in the apical turn, consistent with CS. This suggests that blast exposures to the head such as traumatic brain injuries (TBIs) could potentially be a cause of lower-frequency CS. Alternatively, results from Cho et al. (2013) could point to possible effects of conductive losses on CS. The mice blasted with compressed air exhibited tympanic membrane ruptures with only half of the sample completely healing from the rupture. Similarly, Liberman, Liberman, and Maison (2015) compared mice with conductive hearing loss caused by a lack of tympanic membranes to age-matched mice with typical hearing systems. The researchers showed a loss in cochlear synapses in mice with conductive hearing loss by 64 weeks, either from a missing tympanic membrane or from chronic otitis media. Further potential etiologies for CS include congenital ototoxicity, such as hyperbilirubinemia, which has a high risk factor for auditory synaptopathy in the context of ANSD (Moser & Starr, 2016). Chemotherapy agents such as cisplatin are also known to have ototoxic effects on the hair cells and associated synapses

(Rybak, Mukherjea, Jajoo, & Ramkumar, 2009). Symptoms of chemotherapy-induced ototoxicity include subjective hearing loss, ear pain, or tinnitus (Reddel et al., 1982). However, the present study will aim to investigate noise-induced CS in the context of humans.

Noise-induced hearing loss has been posited as a modern, silent epidemic as it is the second most acquired hearing loss in humans (Imam & Hannan, 2017). As modern sound technology rapidly advances with a lack of regulation or hearing health education, increasing numbers of young people are exposing themselves to dangerous levels of non-occupational loud noise (Johnson, 1993). Discotheque, concerts, and personal music players often grossly exceed the recommended daily noise dose (Mercier & Hohmann, 2002; Sliwinska-Kowalska & Davis, 2012). Noise exposure can lead to TTS (Borg, Canlon, & Engstrom, 1995), which has now been demonstrated by Kujawa & Liberman (2009) to be the result of subclinical, or “hidden”, CS. Indeed, many rock musicians, music club employees, concert attendees, and even orchestra musicians experience TTS immediately following these music events (Dudarewicz et al., 2015; Gunderson, Moline, & Catalano, 1997; Pfeiffer et al, 2007; Yassi et al., 1993). These exposures lead to delayed permanent threshold shifts in high frequencies (Imam, & Hannan, 2017), a pattern that can be attributed to delayed cochlear nerve degeneration that is observed in CS (Kujawa & Liberman, 2009).

1.3 Electrophysiological Assessments of CS

1.3.1 Auditory Brainstem Response Wave I Amplitude

The ABR is an auditory evoked potential reflecting neural activity of the afferent auditory pathway (Picton, 2010). Waveforms elicited by acoustic stimuli are generated by various levels

of the pathway—the first wave (“wave I”) is generated by the synchronous discharge of afferent ANFs making up the cochlear nerve. ANF loss can reach 40-50% before affecting the CAP or ABR wave I amplitude (Bourien et al., 2014). Theoretically, if noise-induced CS primarily affects high-threshold ANFs, then supra-threshold wave I responses could be reduced via cochlear nerve degeneration. This is supported by Kujawa & Liberman (2009), whom demonstrated reduced wave I amplitudes in response to supra-threshold stimuli following traumatic noise exposure but not to stimuli levels at the hearing threshold. Several human studies have also shown reduced wave I amplitudes in individuals with tinnitus despite clinically normal hearing thresholds (Schaette & McAlpine, 2011; Gu, Herrmann, Levine, & Melcher, 2012), further supporting its potential for CS detection. Reduced wave I amplitudes were demonstrated in army veterans with higher lifetime noise exposure compared to younger army members (Bramhall et al., 2017). Similarly, Valderrama et al. (2018) showed a reduced wave I amplitude in adults with higher lifetime noise exposure, although there a large substantial inter-subject variability.

While the wave I is has good test-retest reliability and is a relatively direct measure of cochlear nerve function, human studies within the context of noise-induced CS has yielded conflicting results for its diagnostic utility (Bramhall et al., 2019; Prendergast et al., 2018). The wave I is subject to high variability due to head size, temperature, and electrode distance from the cochlea (Picton, 2010). Stamper & Johnson (2015a, 2015b) showed significantly reduced wave I amplitudes in the high-risk noise exposure group, but only for females. This has been attributed to females on average having a smaller head size than males. Controlling for age and sex, Guest et al. (2017) did not find any differences in Wave I amplitude between high and low

noise exposure groups. Other studies have also noted no significant differences in the wave I amplitudes between high and low noise exposure groups (Grose, Buss, & Hall III, 2017; Guest et al., 2017; Prendergast et al., 2018). On top of the many physiological factors unrelated to CS that may contribute to the variable results, differences in the recording montage, stimuli parameters, and test room conditions can also increase the variability between studies. This underscores a need to develop more sensitive measures for clinical CS identification.

1.3.2 Envelope-Following Response

The envelope-following response (EFR) is a steady-state auditory evoked potential that represents the phase-locking of ANFs and higher order brainstem neurons to the temporal envelope of a carrier sound stimulus (Picton, 2010). At higher stimuli frequencies exceeding the maximum ANF spike frequency, ANF neural spikes will phase-lock to envelope fluctuations. The EFR is a robust, physiological measure that provides information on the fidelity of the auditory system for temporal sound encoding. Temporal sound encoding is important for speech perception and sound localization (see Plack & Oxenham, 2005 for review). A consequence of CS may be a reduced fidelity and precision in temporal coding due to a reduction in both ANF number and synchronous activity (Bharadwaj et al., 2014). Damage to high-threshold ANFs that are preferentially targeted by noise exposure (Furman, Kujawa, & Liberman, 2013) may lead to our supra-threshold temporal envelope coding.

In mice, the EFR of high modulation rates has been shown to predict CS better than the wave I (Shaheen, Valero, & Liberman, 2015). In humans, reduced EFR amplitudes in response to sinusoidal amplitude modulated sounds were observed in participants whom performed worse in

behavioural supra-threshold forced-choice auditory tasks (Bharadwaj et al., 2015). Similar trends were shown in other studies involving participants with tinnitus despite normal hearing thresholds, but these trends did not reach significance (Guest, Munro, & Prendergast, 2018; Paul et al., 2017; Roberts, Paul, & Bruce, 2018). While computational models simulating high-threshold ANF loss showed sufficient differences in AM detection thresholds (Paul, Bruce, & Roberts, 2017), indicating potential sensitivity to CS, EFR remains difficult to test in the context of CS. This is because EFRs cannot be measured easily in humans at the high modulation rates needed in a mouse model (Shaheen, Valero, & Liberman, 2015). As such, diagnostic tools that are more clinically feasible are preferred over the EFR.

1.3.3 Middle Ear Muscle Reflex

The middle ear muscle reflex (MEMR) is believed to be a protective response to loud noise. Loud sound stimuli activates both ipsilateral and contralateral reflex pathways, resulting in the contraction of bilateral stapedius muscles. This contraction serves to dampen the ossicular system. The MEMR has also been proposed to help enhance speech perception in noise by attenuating the transmission of low frequencies over higher frequencies (Katz, 2015; Starr et al., 2001). Theoretically, MEMR strength may be reduced in the presence CS because the MEMR neural circuit involves afferent high-threshold ANFs (Liberman & Kiang, 1984), which are selectively targeted by noise exposure (Furman, Kujawa, & Liberman, 2013). Furthermore, the MEMR has been shown to be absent or reduced in humans with ANSD (Berlin et al., 2005).

The MEMR has been shown to be sensitive to CS in mice (Valero, Hancock, & Liberman, 2016; Valero, Hancock, Maison, & Liberman, 2018). In humans, weaker MEMRs

were seen in those with tinnitus compared to those without tinnitus, irrespective of audiometric thresholds (Wojtczak, Beim, & Oxenham, 2017). However, these results were not replicated when conducted by other research groups (Guest, Munro, & Plack, 2019). From the perspective of using the MEMR for the differential diagnosis of CS, variations in canal resonance between individuals can affect MEMR strength (Bharadwaj et al., 2019). For example, recording the MEMR using a 226 Hz probe tone in a participant with a MEMR spectrum peaks near 226 Hz may result in the false appearance of a weak MEMR compared to participants whose MEMR spectrum peaks outside of 226 Hz. This source of variability lowers the efficacy of the MEMR as a clinical diagnostic tool.

1.3.4 Electrocochleography (ECochG)

Electrocochleography (ECochG) is a technique for recording the bioelectric activity of the cochlea and cochlear nerve. While ABR testing can record reliable cochlear responses, the strength of responses are susceptible to variations in sex and head size, tissue conductivity, and physiological noise. ECochG-recorded cochlear responses are much larger and less susceptible to physiological noise due to the shorter distance of the electrode from the cochlea (Ferraro, 2010). ECochG in the context of CS has been seldom studied. Liberman et al. (2016) used ECochG with a gold-tip ear canal electrode to measure the electrical activity of hair cell potential changes (i.e. summing potential; SP) between individuals with low- and high-risk for noise exposure. They used the SP/CAP ratio commonly used to detect Ménière's disease, and found a larger SP/CAP ratios in the high-risk group. This difference in ratios between groups was driven by the SP. However, similar results could not be replicated by other researchers when using ear canal

(Prendergast et al., 2017a), mastoid (Prendergast et al., 2018), or extra-tympanic (ET) ECochG electrodes (Chang, 2020). While the SP/CAP ratio assess the relationship between hair cell activity and postsynaptic ANF synchrony, it may be more worthwhile to investigate measures that focally target the hair cells upstream from the synapse because of the potential effects of IHC-ANF damage to the efferent system.

1.3.4.1 The Cochlear Microphonic (CM)

The CM is a stimulus-evoked response potential reflecting the electrical activity of hair cells in the cochlea (Shi et al., 2012). CM morphology directly follows the phase of the stimulus, and because it is often elicited using pure tones, the CM is essentially a frequency-following response (Picton, 2010). It can be recorded using either ABR or ECochG methods—although the latter provides more robust CMs due to its closer proximity to the generators (Ferraro, 2010; Picton, 2010). The CM is the sum of both OHC and IHC electric fields, with greater contributions from OHCs because there are far more OHCs than IHCs in the cochlea (Dallos, 1983). An absent or abnormal CM is consistent with alterations to the normal activity of the hair cells (Dallos & Cheatham, 1976; Picton, 2010).

Afferent IHC-ANF dys-synchrony has been proposed to cause prolonged, enlarged CMs through diminished LOC and MOC excitation, and insufficient efferent feedback to the OHCs (Santarelli et al., 2006; Soares et al., 2016). Diminished efferent feedback to OHCs results in decreased hyperpolarization, leaving the OHCs susceptible to feed-forward activation—or a prolonged activation of OHCs. CM amplitudes are believed to be increased by this hyperpolarization as well, with obligatory attenuation of neural activity beyond the cochlea

(Starr et al., 2001). However, Pratt, Sohmer, & Barazani (1978) investigated the effects of noise-induced TTS on the amplitude of the CM using surface electrodes and found no changes to CM amplitude. While the study did not directly investigate CS—the theories of CS and HHL did not exist before the 21st century—it offers some parallel insight since TTS have been shown to result from CS (Kujawa & Liberman, 2009). Through their results, they concluded that the etiology of TTS was likely at the cochlear synapse, and not the hair cells. The efferent MOC feedback system may have a more pronounced impact on the duration of the CM than the amplitude (Santarelli et al., 2016; Smith, 2018), and so investigation of the CM duration may be warranted.

To date, no literature investigating the effects of CS on the CM have been published or made accessible. Current ECochG literature on CS evaluate the SP/CAP ratio as a diagnostic tool (see section 1.3.4). However, as mentioned above in section 1.2.2, CS may be classified as a pathology within ANSD. It could thus be appropriate to review research on CM morphology in ANSD—more specifically, those involving auditory synaptopathies—as a substitute from which parallels can be drawn.

1.3.4.1.1 CM Duration and Amplitude in ANSD

CMs have been characterized as large and long-lasting in cases of ANSD (Berlin et al., 1993; Deltenre et al., 1997; Starr et al., 1991), and is evaluated for differential diagnosis from other cochlear diseases such as cochlear nerve deficiency. Smith (2018) compared ABR-recorded CM duration and amplitude data from infants diagnosed with ANSD to neonatal intensive care and control CM data found by Hunter et al. (2018). CM duration was significantly longer in ANSD infants than compared to control and neonatal intensive care infants from Hunter et al.

(2018). Results also agreed with averaged duration values reported in an ANSD systematic review by Soares et al. (2016). Similarly, Santarelli et al. (2016) found prolonged CM durations in ANSD patients aged 7 months to 47 years compared to normal and central nervous system disorder (e.g. ischemic disorders, congenital malformations, syndromes) patients. CM data in this study was collected using extra-tympanic (ET) and transtympanic (TT) ECochG. These results show promise for the clinical utility of CM duration in ANSD—and potentially CS—diagnosis.

Data on CM amplitude has not been as clear on its viability for ANSD diagnosis. While Starr et al. (2001) found CM amplitudes to decrease with age, corroborating theories of neural maturation effects on the efferent feedback system, they did not find a significant difference in CM amplitudes between ANSD and normal patients. Likewise, Santarelli et al. (2016) did not find meaningful differences in CM amplitudes between the three groups, although it is important to note that CM amplitude can be affected by electrode distance from the cochlear generators (Ferraro, 2010). Santarelli et al. (2016) used peak to trough unnormalized amplitude as their measure, which can be subject to placement and ear canal length variability. However, while Smith (2018) used the CM/CAP amplitude ratio as a normalized amplitude measure, he did not find a significant difference between groups. The researcher posited that the negative results may have been affected by statistical power. Therefore, the CM may still be a potential electrophysiological indicator of auditory synaptopathy identification, and further investigation on its clinical utility is warranted.

As mentioned above, there are several caveats when comparing and interpreting CM studies because the CM morphology can be affected by electrode placement (e.g. ET, TT, scalp surface) and age-related neural maturation (e.g. neural synchrony, myelination, neural pruning).

For example, Santarelli et al. (2006) used TT and ET ECoChG and found a CM mean duration of 6.77 ms (standard deviation: ± 2.58 ms) in ANSD patients (mean age: 3.1 ± 3.9 years), whereas Smith (2018) showed the ABR-recorded CM mean duration to be 4.197 ± 1.154 ms (mean age: 3.5 ± 3.2 months). Differences in recording conditions and age ranges across studies make it difficult to compare, replicate, and draw conclusions on the diagnostic utility of the CM, as well as its clinical utility for CS. *Appendix A.2* lists the different test parameters and CM data for relevant ANSD studies. Despite this, presence of a larger CM in ECoChG studies supports the rationale for using ECoChG over ABR to provide more prominent CM responses. TT ECoChG, while yielding the largest responses due to its proximity to the cochlea, is an invasive procedure that requires surgical insertion of the electrode (Ferraro, 2010). However, ET ECoChG is an accessible alternative, with many commercially available clinical electrophysiological tools providing options for ECoChG assessment.

1.4 Musicians and Noise Exposure

Individuals at high risk of CS are those who experience recurrent exposure to loud noise because noise exposure accumulates over a person's lifetime. In this context, musicians may serve as an appropriate test population for early subclinical hearing damage. Professional musicians often participate in practice sessions and concert performances that exceed recommended sound levels (Chasin, 2009). Studies have found over half of professional orchestral musicians exceed the accepted daily noise dose, with hearing protection during instrument playing activities to be periodic or nonexistent (O'Brien, Driscoll, & Ackermann, 2013; Kardous et al., 2015). Similar findings were found in college music students in the United

States (Wahnsnik et al., 2016). Sound exposure during college band performances and rehearsals have been found to reach average levels of around 89–90 dBA in concert and symphonic bands (Chesky, 2010). Sound exposure levels among professional orchestra members could range 85-97 dBA equivalent continuous sound level (Pawlaczyk-Łuszczynska et al., 2010).

Musicians are at high risk for hearing impairments such as hearing damage, tinnitus, and hyperacusis (Di Stadio et al., 2018; Lüders et al., 2016). Musicians with normal audiometric thresholds are more likely to report hyperacusis, tinnitus, hearing in noise difficulty than non-musicians—even in the younger adult population (Couth et al., 2020). About 57% have persistent ringing or buzzing in the ears (Schink et al., 2014). College music students are likely to experience frequent TTS due to solitary practice and ensemble rehearsals (Gopal et al., 2013). Musicians are also at high risk for sensorineural hearing loss later in life (Di Stadio et al., 2018; Pouryaghoub, Mehrdad, & Pourhosein, 2017; Schmidt et al., 2014). Compared to non-musicians, musicians are four times more likely to develop some level of deafness (Schink et al., 2014). Importantly, CS has been implicated as the underlying cause of these symptoms by many researchers (Hickox & Liberman, 2014; Kujawa & Liberman, 2009; Paul, Bruce, & Roberts, 2017; Plack, Barker, & Prendergast, 2014; Schaette & McAlpine, 2011). Despite this, there is not a lot of literature investigating the auditory system of musicians in the context of CS. Washnik et al. (2020) investigated the CAP amplitude, which is also the wave I, amplitude in music students and found no differences between noise musicians and non musicians. However, they did find a weak negative correlation between noise exposure history and wave I amplitude. Chang (2020) investigated the SP/CAP ratio in music students and found no significant results. If the proposed

theory of efferent feedback disruption in CS is true, and if musicians have a high risk for CS, then further electrophysiological testing upstream from the postsynaptic ANFs is needed.

1.5 Purpose of the Study

Despite the lack of sensitivity in conventional audiometry in the detection of CS, there is currently no standardized clinical battery or protocol for its diagnosis. Various non-invasive measures have been investigated to determine whether noise-induced CS occurs in humans, but the results are conflicting across and between measures (Bramhall et al., 2019). It has been argued that a test battery with a combination of electrophysiological and behavioural tests should be developed to detect CS in humans (Kobel et al., 2017). The present study is part of a larger ongoing research project to develop an accessible clinical test battery for CS diagnosis. Because the mechanisms of CS may create similar efferent system disruptions proposed in ANSD, utilizing a measure employed in the diagnosis of ANSD may provide a promising diagnostic tool for CS. More specifically, if CS reduces ANF communication, it may subsequently reduce efferent MOC-OHC feedback. This could theoretically result in a “runaway” feed-forward system that continually perpetuates cochlear non-linearity via OHC activation—a process that may be observable through hair cell electric activity.

This project investigated the efficacy of the CM, recorded using ECochG, as a physiological measure for the diagnosis of CS. In particular, measures of the CM duration, CM/CAP amplitude ratio (as a measure of normalized amplitude), and overall power were evaluated between music students with a history of noise exposure, and control participants with no prior history of noise exposure. Lifetime noise exposure was evaluated using the Noise Exposure

Structured Interview (NESI). The purpose of the present study is to determine the efficacy of ECochG for HHL, with hopes to improve current standard audiological evaluations such that HHL may no longer be hidden.

1.6 Hypothesis

H1: CM duration is significantly longer in individuals with a high risk of noise exposure than normally-hearing individuals.

H2: CM/CAP amplitude ratio is significantly larger in individuals with a high risk of noise exposure than normally-hearing individuals.

H3: CM power is significantly larger in individuals with a high risk of noise exposure than normally-hearing individuals.

Ho1: CM duration is not significantly different between individuals with a high risk of noise exposure than normally-hearing individuals.

Ho2: CM/CAP amplitude ratio is not significantly different between individuals with a high risk of noise exposure than normally-hearing individuals.

Ho3: Normalized CM power is not significantly different between individuals with a high risk of noise exposure than normally-hearing individuals.

Chapter 2: Methods

2.1 Data Source

The current study was a retrospective analysis of ET electrocochleography (ECochG) data collected in the Middle Ear Laboratory at the University of British Columbia. The data was originally collected for research by Chang (2020), who investigated the effect of CS on the ECochG-recorded SP/CAP ratio of the Wave I.

The parent study from which the ECochG data were drawn was designed to investigate the efficacy of behavioural and physiological measures for the clinical diagnosis of CS. Recruited participants were asked to complete a case history followed by a screening session to confirm eligibility for the parent study. Hearing screening consisted of otoscopic examination and air-conduction pure-tone audiometry (250-16,000 Hz). Participant audiometric thresholds were obtained using the automatic Békèsy method, with pulsed tones in 1 dB steps, from an Madsen Astera² audiometer (Natus, United States). Qualifying participants (see section 2.2.1 and section 2.2.2 below) subsequently completed the following test battery of behavioural, physiological, and speech comprehension assessments: Tinnitus Handicap Inventory, acoustic reflexes, wideband tympanometry, transiently-evoked and distortion product OAEs, contralateral suppression of OAEs, NESI, loudness scaling, Threshold in Noise 21 test (TEN), Multiple Auditory Processing Assessment (MAPA), Temporal Modulation Transfer Function, triple digits in noise, Hearing In Noise Test (HINT), random gap detection test, and ECochG. For the purpose of the present study, this paper will solely focus on the NESI and ECochG data collected from the test battery.

2.2 Subject Records

Records from a total of 37 subjects (27 female, 10 male) were obtained. Of these subjects, 18 music students (14 female, 4 male) with a history of career-related noise exposure and confirmed normal hearing thresholds were recruited for the high-risk group. Music students were recruited through the Department of Music at the University of British Columbia because of their regular exposure to musical instruments, often without hearing protection. The other 19 participants (13 female, 6 male) were non-musicians with normal hearing and recruited for the low-risk control group. All subject records included a quantified lifetime noise exposure history using the NESI, developed by Guest, Dewey, Plack, et al. (2018).

ECochG data were recorded using two Interacoustics Eclipse system softwares version 4.4 and version 4.5 Research Module), which were then stored in the Interacoustics OtoAccess database (Demant, Denmark). Records stored in the OtoAccess database via the Eclipse version 4.5 with a Research Module license (high-risk: 16; control: 9) were extracted to Matlab format using custom software and then used for further analyses.

2.2.1 Inclusion Criteria

Groups were defined as high risk (music students) and low risk (control group) to ear damage. Each participant was recruited to an assigned group based on whether they were a music student or not. All participants fell within the following criteria:

- 1) No history of head trauma or concussions
- 2) Air conduction thresholds between 250 Hz and 8000 Hz less than or equal 25 dB HL

- 3) No asymmetry in air conduction thresholds—defined as a difference of more than 15 dB HL at one frequency—between the left and right ear from 250 Hz to 8000 Hz
- 4) No active middle ear involvement or excessive cerumen present
- 5) Presence of OAEs in at least three out of five standard frequencies in either the distortion product OAEs or transiently evoked OAEs, and the mandatory presence of either OAE at 4000 Hz
- 6) Overall usage of personal listening devices equal to or below 60% volume as recommended by the World Health Organization (2015)

Additionally, participants in the control group were required to further satisfy the following criteria:

- 1) No history of tinnitus, ear injury, ear surgery, or recent ear infections
- 2) No asymmetry in air conduction thresholds between the left and right ear from 9000 Hz to 16,000 Hz
- 3) No history of loud noise exposure

2.2.2 Exclusion Criteria

ECochG recordings were not collected if participants had excessive cerumen present in the ear canal. Two ears in the high-risk group and two ears from the control group were excluded from data collection in the original study due to excessive cerumen. In the present study, unilateral data were rejected from analyses if the files had electrical noise that impeded the visual interpretation and labeling of waveform peaks. Data from two ears in the high-risk group and one ear from the control group were excluded due to excessive noise in the recordings, likely from

external electrical interference in a non-shielded test room. An additional ear from both the high-risk group and control group were excluded from analysis because the exported files did not contain waveform data. As binaural data was not a requirement for the present study, participants with unilateral data rejections were still eligible for data analysis. In total, 16 participants (n = 27 ears) comprised the high-risk group (mean age: 21.75 ± 2.46 years; range 18-26 years), and 8 participants (n = 14 ears) comprised the control group in the present study (mean age: 22.25 ± 3.20 years; range: 18-28 years).

	High-risk	Control
	Participants	
Female	12	6
Male	4	2
Total	16	8
Mean age (yrs)	21.75	22.25
SD	2.46	3.20
Age range	18-26	18-28
	Ears	
Female	22	10
Male	5	4
Total	27	14

Table 2.1 Demographic summary of participants included in analysis.

2.3 Lifetime Noise Exposure History

Noise exposure history from each participant was recorded for the original study using the Guest, Dewey, Plack, et al. (2018) NESI questionnaire. The questionnaire provided a quantified estimate of the noise exposure based on the participant's self-reported vocal effort during every notable activity in their lifetime. The NESI was implemented in an open-answer interview style to elicit relevant noise exposure history without restricting the participant to pre-determined activities. The NESI also accounted for lifestyle changes throughout one's lifetime. Participants were asked to list every noisy recreational and occupational activities in which they participated throughout their lifetime. Noisy activities were defined by the participant's perceived need to raise their voice for communication during such events, and were estimated to be ≥ 80 dB SPL. One converted unit of NESI was equivalent to one working year of noise exposure to 90 dBA. The raw NESI units were used in analysis as a measure of the participant's cumulative lifetime noise exposure history.

2.4 ECochG Procedure

ET ECochG data used in the present study were recorded by Chang (2020) in either a quiet room at the Middle Ear Laboratory or in a sound-attenuated, electrically-shielded sound booth at the BRANE Laboratory. Both laboratories are located at the University of British Columbia. Participants were lying supine on a bed or reclining chair for the duration of the recording. Target areas of the skin were prepped for surface recording electrodes in a horizontal montage. The active non-inverting electrode was placed on the contralateral mastoid and the ground electrode was placed at the centre midline of the forehead. Both the participant's ear

canal and an ET Lilly TM-Wick electrode (Intelligent Hearing Systems, United States) were soaked in saline for increased conductivity. The tip of the ECochG electrode was then dipped in electrode gel and placed on the ipsilateral tympanic membrane surface. Impedance between electrodes were ≤ 25 k Ω . Otoscopic examination was conducted pre- and post-procedure to ensure tympanic membranes were intact. The protocol was repeated using the same ET electrode for each participant's opposite ear.

ECochG stimulus generation and data collection were conducted using an Eclipse EP25 hardware system and version 4.5 software with a Research Module license. An EP4A amplifier was used. Acoustic stimuli were delivered via Etymotic Research (ER)-3A earphones using plastic sound tube and foam tip inserted in the ear canal. Broadband click stimuli (200-11,000 Hz; 100 μ s) were delivered at 95 dB nHL (130.5 dB SPL) at a rates of 11.3 Hz and 88.8 Hz. Responses to a higher click rate were collected because click rates above 70 Hz is known to decrease the amplitude of waves I-V while the CM amplitude remains unaffected (Picton, 2010). Rarefaction click (RC) and condensation click (CC) stimuli were presented in separate trials and later averaged offline to obtain an alternating polarity waveform. Stimulus polarity was reversed for separate trials to confirm the presence of the CM because the CM follows the inversion of the stimulus while the neural wave I-V components do not (Soares et al., 2006; Picton et al., 2010). No contralateral masking stimulus was used during click stimulus presentation. Electrical responses were amplified by 40,000x and bandpass filtered between 3.3-5000 Hz. Responses to 1000 stimulus repetitions (1000 sweeps) were recorded from 2 ms pre-stimulus to 12 ms post-stimulus for each waveform. The online rejection criterion was ± 40 microvolts (μ V). Two rarefaction and two condensation replications of 1000 sweeps was recorded for each ear. A

baseline “clamped” replication of 1000 sweeps in RC polarity was additionally recorded by blocking sound transmission from passing through the ER-4A sound tube. This was done by clamping the tube with a plastic medical tubing clamp during recording. Clamping of the sound tube was performed to prevent the acoustic signal of the click stimulus from travelling to the ear, while still sending the electrical signal to the transducer so that the electrical stimulus artifact can be recorded. These “clamped” tube replications allowed for visualization of stimulus artifact waveforms that can sometimes ring within the interval window of when the CM occurs. Thus, the clamped-tube replications were performed as a control to confirm the CM is larger than the stimulus artifact and therefore a true physiological event. In an effort to minimize stimulus artifact, caution was taken to ensure electrode wires did not make contact with transducers during recordings.

2.5 Waveform Analysis

Waveform analyses were performed separately for each ear. Exported Eclipse data files were imported to a simulated auditory brainstem response (sABR) software (University of British Columbia, Canada), a MatLab program created by Dr. Anthony Herdman. The software used in the present study is a custom research version of the sABR program (v10.3) created in May 2020 for retrospective waveform analysis.

In sABR 10.3, the time window (x-axis) was set from -2 ms to 10 ms and the amplitude scale was set from 0 μV to anywhere between 8-20 μV . Various mathematical operations were carried out on the imported data files, which are shown in order from top to bottom for a typical ear in *Figure 2.1*. Offline sweeps-weighted averaging was performed on two RC waveforms and

two CC waveforms elicited using 11.3 Hz click stimuli (*Figure 2.1a*). An overlay of the two averaged waveforms of opposite polarity allow the CM to be displayed. The two resulting waveforms were then further averaged to produce an alternating waveform (*Figure 2.1b*). The alternating waveform revealed neural components present in the RC and CC recordings that could affect accurate waveform labelling, while eliminating the oscillatory, phase-inverted CM components. An amplitude-weighted subtraction was then performed on the average RC waveform by the averaged CC waveform, and the difference multiplied by 0.5. This was performed in case RC or CC replications had different number of recorded sweeps. The product is a RC-CC/2 waveform, shown as RC-CC in *Figure 2.1c*. By contrast to the alternating waveform, subtracting the RC polarity waveform with the CC polarity waveform eliminates non-inverting neural potentials. The RC-CC/2 waveform, when overlaid with the CC-RC/2 waveform achieved by multiplying RC-CC/2 by -1, allowed the phase-inverting CM to be best visualized for labelling. Raters were tasked to make a conservative (III marker's latency) and liberal (IV marker's latency) judgement of the CM duration. The duration of the CM oscillation was judged to be a time point of visual oscillation onset to the point when the oscillation is no longer visible. The CM amplitude was calculated as the largest identified peak-to-peak oscillation within the conservative (CM-CM' marker amplitude) and liberal (II-II' marker amplitude) (*Figure 2.1c*). The difference waveforms provided a better visualization of the CM response because the auditory neural responses have been mostly subtracted from the waveform.

The operations performed were then repeated on waveforms with 88.8 Hz click stimuli, and the phase-inverting RC-CC/2 and CC-RC/2 were plotted (*Figure 2.1d*). The 88.8 Hz data provided visual aide for the labelling of CM components on 11.3 Hz waveforms as the neural

components are significantly diminished when presenting higher click rate stimuli (Picton, 2010). The clamped-tube replications in RC and CC polarity were additionally collected for each ear to distinguish stimulus artifacts from a CM response and aide in the labelling process (*Figure 2.1e*). If a CC clamped-tube replication was not available, the RC clamped-tube replication was multiplied by -1 to mimic the CC clamped-tube replication.

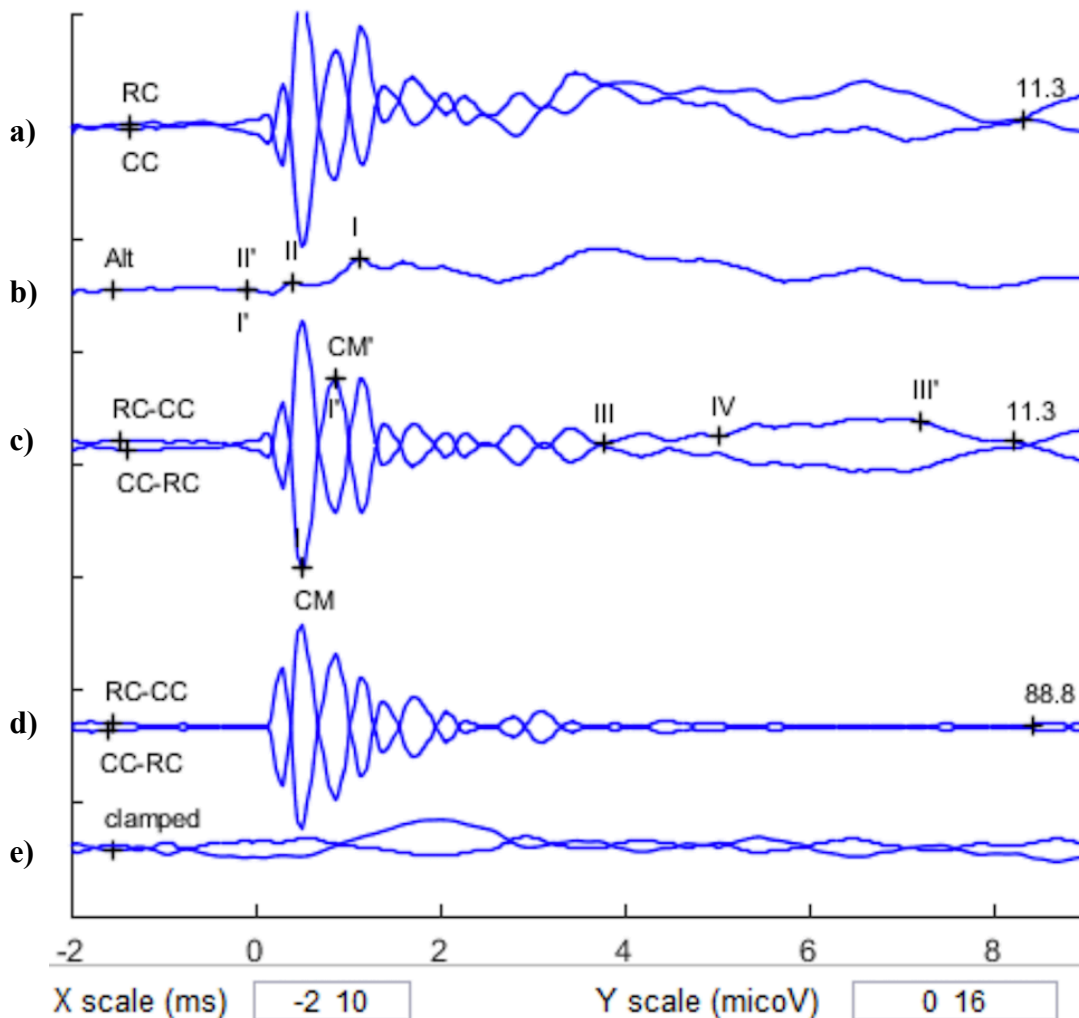


Figure 2.1 Typical waveform averaging on a high-risk participant, obtained from sABR v10.3. Averages are sweeps-weighted, while subtractions are amplitude-weighted. *a)* Averaged RC and CC waveforms recorded in response to 11.3 Hz click stimuli, overlaid to display phase-inverted CM oscillations. *b)* Alternating waveform response to 11.3 Hz stimuli with the CM eliminated to show non-inverting neural components. AP and SP amplitudes labelled I-I' and II-II', respectively. *c)* Difference waveform RC-CC achieved by subtracting the averaged CC from the averaged RC waveform and multiplying by 0.5. CC-RC waveform achieved by multiplying the RC-CC waveform by -1. Non-inverting neural components have been eliminated from both overlaid tracings to show the CM. Responses to 11.3 Hz stimuli. Conservative and liberal estimates of CM duration labelled III and IV. Peak-to-trough CM amplitude labelled CM-CM'. *d)* RC-CC and CC-CC waveform responses to 88.8 Hz click stimuli. Achieved using the same calculations from *c)* waveforms. *e)* Clamped-tube tracings with the CM and non-inverting neural components eliminated. Inverted clamped-tube tracing achieved by multiplying the recording by -1.

2.5.1 CM Duration Measurement

The CM duration was defined as the interval from the onset time of the initial oscillatory phase reversal to the time at which the oscillatory phase reversals completely decayed and were no longer visually apparent (Hunter et al., 2018; Shi et al., 2012). In the present study, CM waveforms roughly began around the 0 ms time period, and thus only the endpoint of the CM phase reversals was labelled to measure its duration. The CM duration values were measured by three raters, whom were instructed to visually identify the CM endpoint as the point at which the CM waveform oscillation stopped decaying in an exponential manner or that the phase reversals of the RC and CC waveforms were no longer apparent. The raters were asked to do this for a conservative and liberal internal criterion. Because CM duration is difficult to identify within noisy ECoG waveforms, having conservative and liberal judgements provided some control over subjective biases among raters. Identical liberal and conservative values for a participant ear were possible if the rater was certain of the CM endpoint. The two values were analyzed separately for significance.

CM duration was measured from the RC-CC/2 difference waveform overlaid on the CC-RC/2 waveform. Waveforms were lined up by the pre-stimulus tracings as much as visually possible. The endpoint of the CM was labelled at a point where the difference waveforms intersected. Due to the decaying nature of the CM amplitude across time, the CM amplitude was not expected to grow at a later point in its duration. As such, spontaneous amplitude growth later in the waveform was assumed to be either artifact or neural component differences between RC and CC stimuli. These events were excluded from labelling at the discretion of the rater.

To help determine if the later oscillations are due to neural component differences in CC and RC stimuli, difference waveforms from 88.8 Hz click stimuli were overlaid under the difference waveforms from 11.3 Hz click stimuli. This also served to aid in the approximation of the CM duration. Stimulus rate changes from 11.3 to 88.8 Hz can significantly reduce neural amplitudes (Picton, 2010). Thus, if differences between CC and RC stimuli were reduced in the 88.8 Hz recordings then those oscillations in the RC-CC waveforms were deemed to be neural components and not from the CM. This allowed a more accurate measure of the CM morphology and duration. The clamped-tube tracing further aided in CM identification by revealing large stimulus artifacts that were present in the waveforms. If stimulus artifacts continued into the post-stimulus time interval and were larger than the possible CM oscillation, then that recording was rejected from further analyses.

2.5.2 CM Amplitude Measurements and CM/CAP Amplitude Ratio

The amplitude of the CM was also measured from the RC-CC/2 difference waveform. The CM amplitude was determined to be within the measured CM duration. CM amplitude was defined as the absolute value from the most positive deflecting peak, to the most negative deflecting adjacent trough past the baseline, without an intervening positive going deflection. Both a liberal and conservative CM amplitude value were measured for each participant and ear, and were calculated from the liberal and conservative CM duration intervals, respectively. Identical liberal and conservative peak-to-trough values for a participant ear were possible.

The alternating polarity waveform was used to measure the peak amplitude of the CAP. The CAP, also known as the Wave I, was defined as the largest positive peak after 1 ms (Picton,

2010). CAP amplitude was calculated from the most positive peak relative to the pre-stimulus baseline. The absolute CAP and CM values were used to calculate the CM/CAP amplitude ratio. The CAP amplitude was used as normalization for the CM values to control for amplitude variability between participants due to insertion depth. Insertion depth has a known effect on amplitude—the closer the electrode to the generator, the larger the response (Ollick, 2016; Picton, 2010). Amplitude values were measured in μV .

2.5.3 CM Power

The area under the curve of the CM was calculated via Matlab software to provide a measure of its power, or energy over time (*Figure 2.2*). CM power was calculated by rectifying and summing the amplitudes (i.e. calculating total area) of the RC-CC waveforms above $0 \mu\text{V}$ (*Figure 2.2b*), within the interval between 0 ms and the rated CM duration latency, and then dividing by the rated CM duration. The CM power is presented in units of Watts, which represents a measurement of the rate of energy per unit time. Because CM amplitude can vary by a function of the TM electrode insertion depth (see section 2.5.2), the CM power was normalized to the CAP amplitude. Both liberal and conservative calculations of normalized CM power were obtained for statistical analysis.

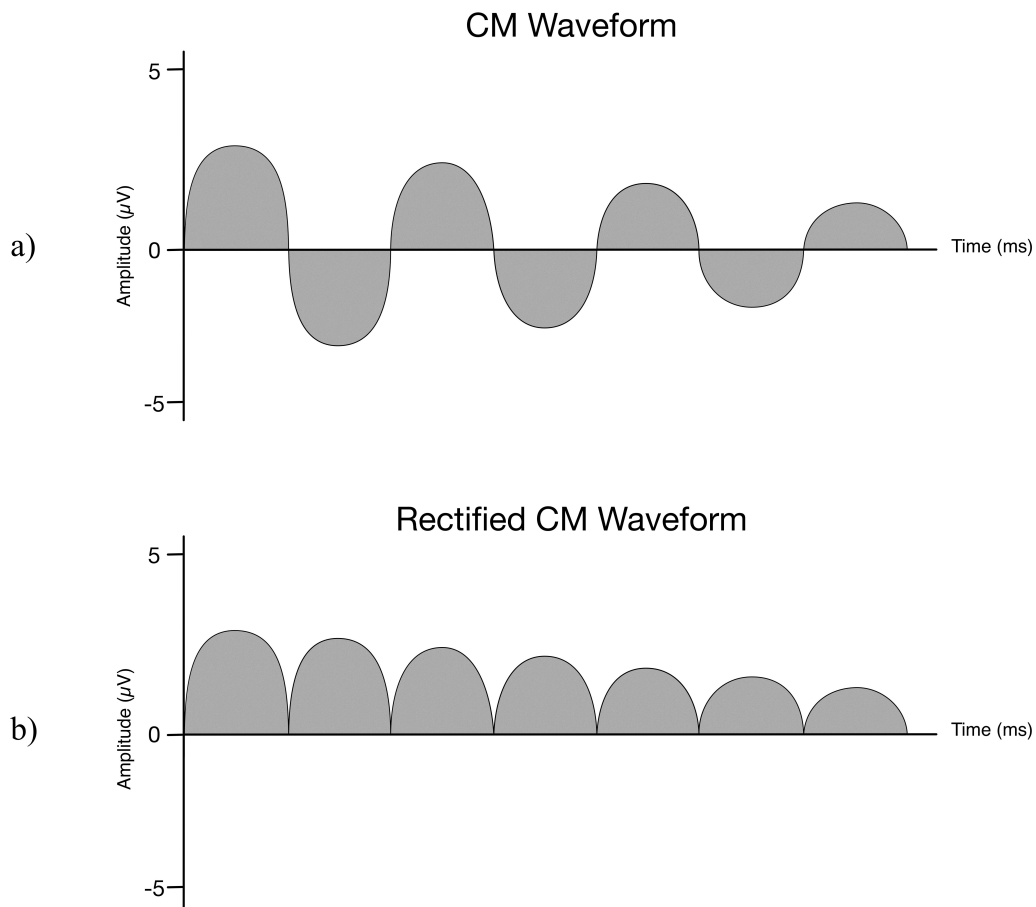


Figure 2.2 CM power calculated by summing the area under the curve, and dividing by the rater-defined CM latency under liberal or conservative criteria. Area under the curve is calculated by a) taking the CM waveform from 0 ms to the rater-defined CM latency and b) rectifying the waveform such that all values are above 0 μV .

2.5.4 Raters

Waveform measurements were performed by three trained personnel from the BRANE Lab. Data was de-identified and given randomized identification codes to prevent rater bias. The researcher of the present study performed all mathematical operations on the data source using sABR v10.3, and then saved the manipulated waveforms as templates for labelling by all raters.

Three raters were provided these templates to label, which eliminated variability in how waveforms were overlaid. This was especially important for the identification of the CM duration, which was labelled at the first data point where both difference waveforms intersected.

2.6 Statistical Analysis

Statistical analyses were performed on CAP measures (latency and baseline-to-peak amplitude), conservative CM measures (amplitude, latency, and power), liberal CM measures (amplitude, latency, and power), and CM/CAP ratios. SPSS Statistics software version 26 (IBM, United States) was used to perform all statistical analyses. A p-value <0.0083 (Bonferroni, $0.05/6$) was considered to be statistically significant for the present study.

Left and right ear data were combined for all groups. A one-tailed Welch's t-test was used to analyze the effect of music background on lifetime noise exposure for small and uneven sample sizes. Group (high-risk versus control) served as the independent variable, and NESI scores served as the dependent variable. A repeated-measures analysis of variance (ANOVA) design was used to analyze the effects of music background and rater on the ECochG measures. In this model, group (high-risk, control) served as the categorical factor, raters served as the repeated measure, and the CM/CAP amplitude ratio, CM duration, and normalized CM power in Watts served as dependent variables. Pearson's r correlations were performed as a measure of inter-rater reliability. Pearson's r correlation tests were also performed between NESI scores and all CM measures, in liberal and conservative, to test the relationship between music background and the CM.

Chapter 3: Results

3.1 Lifetime Noise Exposure History

Each participant's noise exposure history was recorded for the original study using the NESI and calculated into raw scores to quantify the participants' estimated lifetime noise exposure. One NESI unit was equivalent to one working year of exposure to 90 dBA. There was no evidence for a significant effect of group on NESI scores ($t(39) = -1.862, p = 0.037$), although the results trended toward significance (*Figure 3.1*). Interestingly, if an uncorrected p-value <0.05 was used, there would be evidence that the musicians had significantly higher NESI scores than non-musicians. The descriptive statistics of NESI scores are shown in *Table 3.1*.

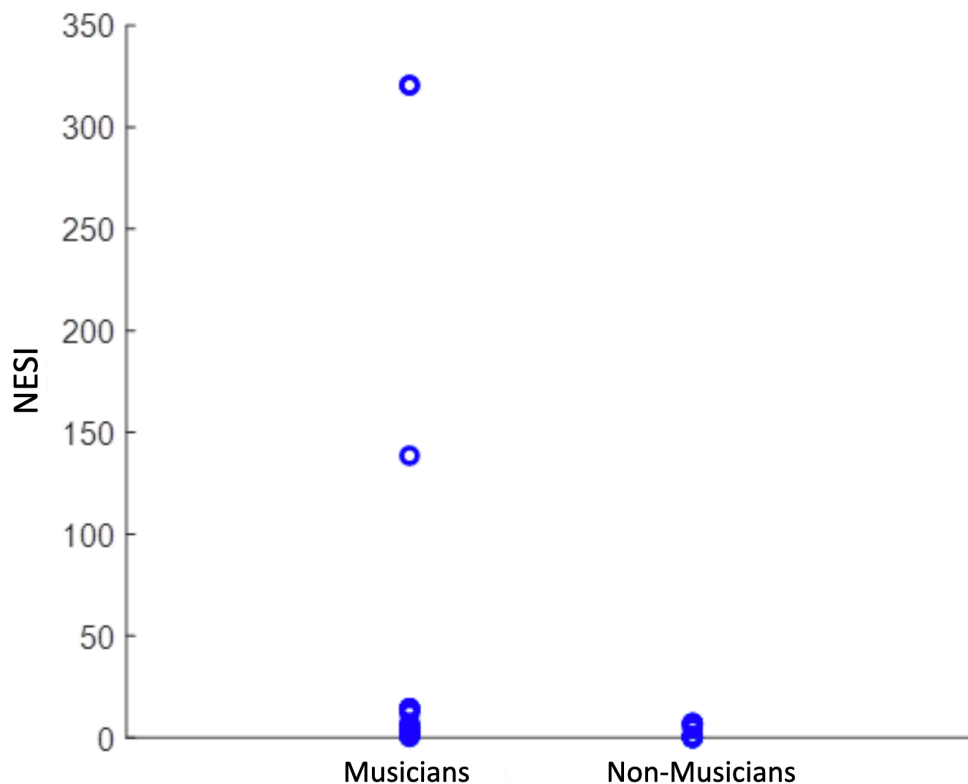


Figure 3.1 Scatterplot for all NESI scores between the high-risk musician group and control non-musician group. Raw NESI scores are plotted along the x-axis. No significant differences were found in NESI scores between groups ($t(36) = -1.862, p = 0.037$).

Raw NESI Scores (All Participants)		
	High-risk	Control
Median	3.83	0.48
Mean	33.56	2.44
SD	86.73	3.13
Minimum	0.34	0.06
Maximum	320.61	7.15

Table 3.1 Mean, standard deviation, minimum, and maximum recorded units of noise exposure for high-risk and control groups.

For statistical analyses involving NESI scores, three participants were not included as their NESI scores appeared to be outliers that heavily skewed results. The three raw NESI scores were much higher relative to raw scores of the group sample and were impractical representations of a young adult's noise exposure (i.e. 320.61 years of 90 dBA noise for the maximum NESI score). Therefore, these were determined to not be representative of the sample population. The abnormally high scores may have resulted from subjective participant interpretation of loudness for each noisy activity (see Supplementary Material 2 from Guest et al. (2018) for the estimated noise level chart). NESI scores excluding outliers are plotted in *Figure 3.2*. Excluding outlier data, there was no evidence for a significant effect of group on NESI scores ($t(36) = -2.192, p = 0.0175$). However, the results reached near significance. *Figure 3.2* shows the distribution of NESI scores in the high-risk group compared to the low-risk group. Interestingly, if an uncorrected p-value of <0.05 was used, there would be evidence that the musicians had significantly higher NESI scores than non-musicians. The descriptive statistics of NESI scores excluding outliers are shown in *Table 3.2*.

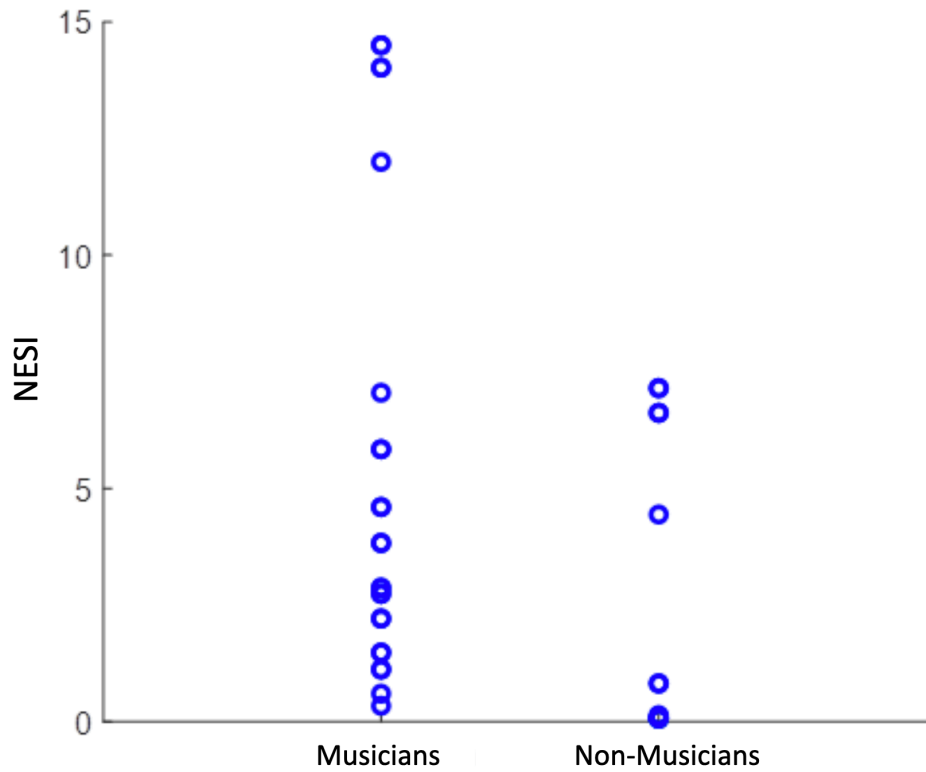


Figure 3.2 Scatterplot of NESI scores, excluding outliers, between the high-risk musician group and control non-musician group. Raw NESI scores are plotted along the x-axis. No significant differences were found in NESI scores between groups ($t(36) = -2.192, p = 0.0175$), however results trended towards significance.

Raw NESI Scores (Excluding Outliers)		
	High-risk	Control
Median	3.35	0.48
Mean	5.27	2.44
SD	4.80	3.13
Minimum	0.34	0.06
Maximum	14.50	7.15

Table 3.2 Mean, standard deviation, minimum, and maximum recorded units of noise exposure for high-risk and control groups excluding outliers.

Pearson correlation coefficients were computed to test the relationship between raw NESI scores and each measured component of the waveforms (*Table 3.3*). No evidence of statistically significant relationships found between NESI scores and CM duration, CM/CAP amplitude ratio, nor CM power for liberal or conservative criteria. Therefore, NESI scores did not predict an increase or decrease of these measured values.

NESI Pearson Correlation Coefficients			
	Rater 1	Rater 2	Rater 3
CM Power (con)	0.001 ($p = 0.498$)	-0.009 ($p = 0.478$)	-0.038 ($p = 0.410$)
CM Power (lib)	0.009 ($p = 0.478$)	0.011 ($p = 0.475$)	-0.019 ($p = 0.456$)
CM Duration (con)	-0.031 ($p = 0.427$)	0.004 ($p = 0.491$)	0.071 ($p = 0.335$)
CM Duration (lib)	0.091 ($p = 0.293$)	0.108 ($p = 0.259$)	0.122 ($p = 0.233$)
CM/CAP Amplitude (con)	-0.114 ($p = 0.247$)	-0.083 ($p = 0.310$)	-0.092 ($p = 0.291$)
CM/CAP Amplitude (lib)	-0.095 ($p = 0.286$)	-0.101 ($p = 0.274$)	-0.091 ($p = 0.293$)

Table 3.3 Pearson correlations ($r(38)$) between NESI and the CM power, CM duration, and CM/CAP amplitude ratio measures for both conservative (con) and liberal (lib) criteria. Bolded values represent significant relationships.

3.2 Electrophysiological Measurements

Table 3.4 displays mean and standard deviation values for CM duration, CM/CAP amplitude ratio, and CM power—under both liberal and conservative criteria. The table is divided by rater and group. Further descriptive statistics are included in *Appendix B Table B.1* to *B.3*.

	High-risk		Control	
Rater 1	Mean	SD	Mean	SD
CM Duration (lib)	3.4474	0.9341	3.2193	0.7352
CM Duration (con)	2.7589	0.8809	2.7936	0.7541
CM/CAP Amplitude (lib)	1.9414	1.9244	1.0226	0.7535
CM/CAP Amplitude (con)	1.9300	1.9310	1.0770	0.7066
CM Power (lib)	0.00094	0.00075	0.00101	0.00066
CM Power (con)	0.00085	0.00072	0.00090	0.00055
Rater 2	Mean	SD	Mean	SD
CM Duration (lib)	3.250	1.306	2.926	1.247
CM Duration (con)	1.755	0.916	1.555	0.874
CM/CAP Amplitude (lib)	1.876	1.758	0.992	0.657
CM/CAP Amplitude (con)	1.801	1.809	0.859	0.683
CM Power (lib)	0.00086	0.00071	0.00093	0.00075
CM Power (con)	0.00051	0.00062	0.00078	0.00061
Rater 3	Mean	SD	Mean	SD
CM Duration (lib)	4.7378	1.2478	4.8171	1.1137
CM Duration (con)	2.7496	1.0040	2.5221	0.6345
CM/CAP Amplitude (lib)	1.7825	1.8854	0.9634	0.5597
CM/CAP Amplitude (con)	1.8725	1.8208	0.9837	0.5949
CM Power (lib)	0.00112	0.00068	0.00109	0.00057
CM Power (con)	0.00080	0.00054	0.00084	0.00054

Table 3.4 Mean and standard deviation of measured values for high-risk and control groups.

3.2.1 CM Duration

Each rater measured two CM duration values for each participant—one under liberal criteria and one under conservative criteria. The measured CM duration values are plotted in *Figure 3.3*. Each rater was labelled by colour, with liberal and conservative values plotted separately by group.

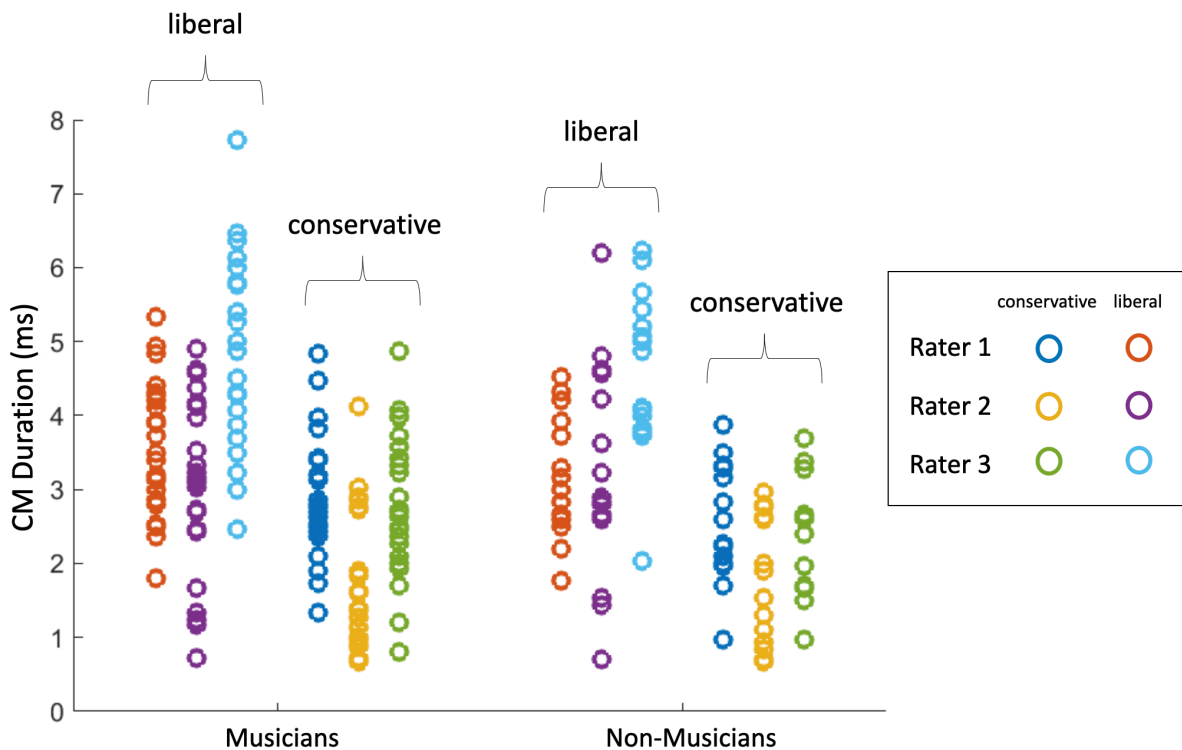


Figure 3.3 Scatterplot of measured CM duration values from three raters between the high-risk musician group and control non-musician group. Measured values under conservative and liberal criteria are shown separately. CM duration is plotted along the x-axis in ms. Groups were plotted along the y-axis.

Distribution of liberal CM duration values were visually similar between groups, with the data points in the high-risk group overlapping data points from the low-risk group. A two-way repeated measures ANOVA showed no significant main effect of group on liberal CM duration

($F_{1, 39} = 0.352, p = 0.557, \eta_p^2 = 0.009$), and no significant interaction between group and raters' values ($F_{2, 78} = 0.427, p = 0.654, \eta_p^2 = 0.011, GG = 0.862$). There was a significant main effect of rater on measured CM duration value ($F_{2, 78} = 32.074, p = 0.000, \eta_p^2 = 0.451, GG = 0.862$), indicating a difference between raters when evaluating the same participants' CM responses. The inter-rater reliability was tested to evaluate the replicability of CM duration values across raters. Inter-rater reliability was quantified using Pearson r correlations between each possible pair of raters and by collapsing across group. Raters 1 and 2 showed a weak positive correlation that was significant ($r(41) = 0.498, p = 0.001$), however neither showed a significant correlation with rater 3 ($r(41) = 0.024, p = 0.444; r(41) = 0.141, p = 0.199$). A table of Pearson's r and p values for inter-rater reliability is shown in *Appendix A.1*.

Likewise to the liberal values, the conservatively measured CM durations overlapped between the high-risk and low-risk groups. Both groups had visually similar distributions, and statistical analysis showed no significant main effect of group on conservative CM duration ($F_{1, 39} = 0.378, p = 0.542, \eta_p^2 = 0.010$), nor a significant interaction between group and rater's results ($F_{2, 78} = 0.358, p = 0.700, \eta_p^2 = 0.009, GG = 0.963$). There was a significant main effect of rater on CM duration values ($F_{2, 78} = 25.717, p = 0.000, \eta_p^2 = 0.397, GG = 0.963$). Inter-rater reliability was computed using Pearson's r correlations. Inter-rater reliability between raters 1 and 2 showed a weak positive correlation that would have been significant if p-value < 0.05 was not Bonferroni-corrected ($r(41) = 0.299, p = 0.034$). Neither raters showed a significant correlations with rater 3 ($r(41) = 0.220, p = 0.092; r(41) = 0.157, p = 0.173$).

3.2.2 CM/CAP Amplitude Ratio

The CM/CAP amplitude ratio was calculated using CM and CAP amplitudes measured by each rater. Similar to the CM duration, each rater was instructed to measure these values under liberal criteria as well as conservative criteria. Distribution of these data points are plotted in *Figure 3.4*. Each rater was labelled by colour with liberal and conservative values shown plotted separately.

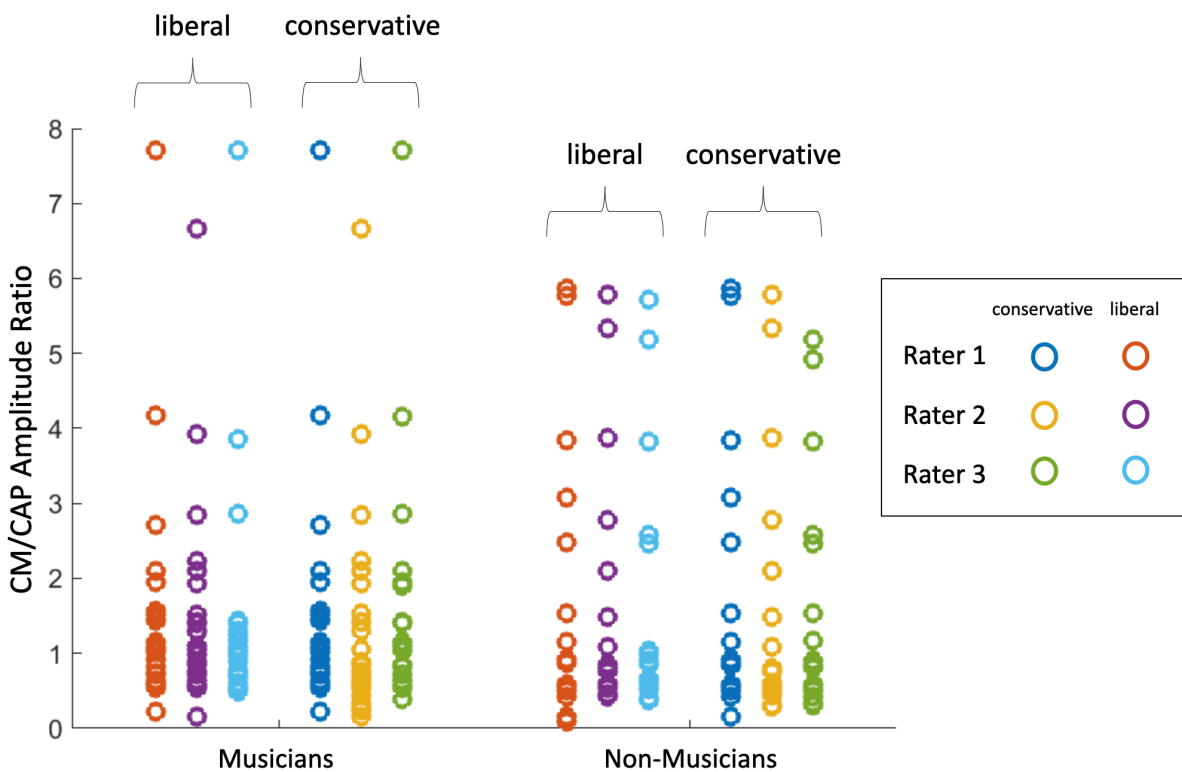


Figure 3.4 Scatterplot of calculated measured CM/AP amplitude ratio values from each rater between the high-risk musician group and control non-musician group. Measured values under conservative and liberal criteria are shown separately. CM/CAP ratios were plotted along the x-axis. Groups were plotted along the y-axis.

Visual distribution of CM/CAP amplitude ratios showed that the majority of ratios fell under a value of 2. Amplitude ratio values were similar within groups among liberal and

conservative measures, indicating that amplitude values were judged to be similar between liberal and conservative criteria. The distribution of amplitude ratios was visually similar between groups, with the data points in the high-risk group overlapping data points from the low-risk group. A two-way repeated measures ANOVA showed no significant main effect of group on liberal ($F_{1, 39} = 2.920, p = 0.095, \eta_p^2 = 0.070$) or conservative CM/CAP amplitude ratios ($F_{1, 39} = 3.060, p = 0.088, \eta_p^2 = 0.073$). No evidence was found for a significant main effect of rater on liberal CM/CAP amplitude ratios ($F_{2, 78} = 2.145, p = 0.124, \eta_p^2 = 0.052, GG = 0.889$) but a significant effect was found for conservative CM/CAP amplitude ratios ($F_{2, 78} = 7.073, p = 0.002, \eta_p^2 = 0.154, GG = 0.916$). Also, no evidence was found for a significant interaction between group and raters on liberal ($F_{2, 78} = 0.460, p = 0.633, \eta_p^2 = 0.012, GG = 0.889$) or conservative ratios ($F_{2, 78} = 0.479, p = 0.621, \eta_p^2 = 0.012, GG = 0.916$).

Inter-rater reliability was computed using Pearson's r correlations to evaluate how raters judged CM and CAP amplitudes relative to each other. Under liberal criteria, all raters showed a strong positive correlation that was significant ($r(41) = 0.991, p = 0.000; r(41) = 0.980, p = 0.000; r(41) = 0.976, p = 0.000$). Likewise, under conservative criteria all raters showed a strong positive correlation that was significant ($r(41) = 0.986, p = 0.000; r(41) = 0.980, p = 0.000; r(41) = 0.976, p = 0.000$). A table of Pearson's r and p values for inter-rater reliability is shown in *Appendix A.1*.

3.2.3 CM Power

The CM power was calculated using MatLab software taking the area under the CM waveform up to the liberally or conservatively defined CM duration, then dividing by its

duration. Distribution of these data points are plotted in *Figure 3.5*. Each rater was labelled by colour, and the liberal and conservative values were plotted separately.

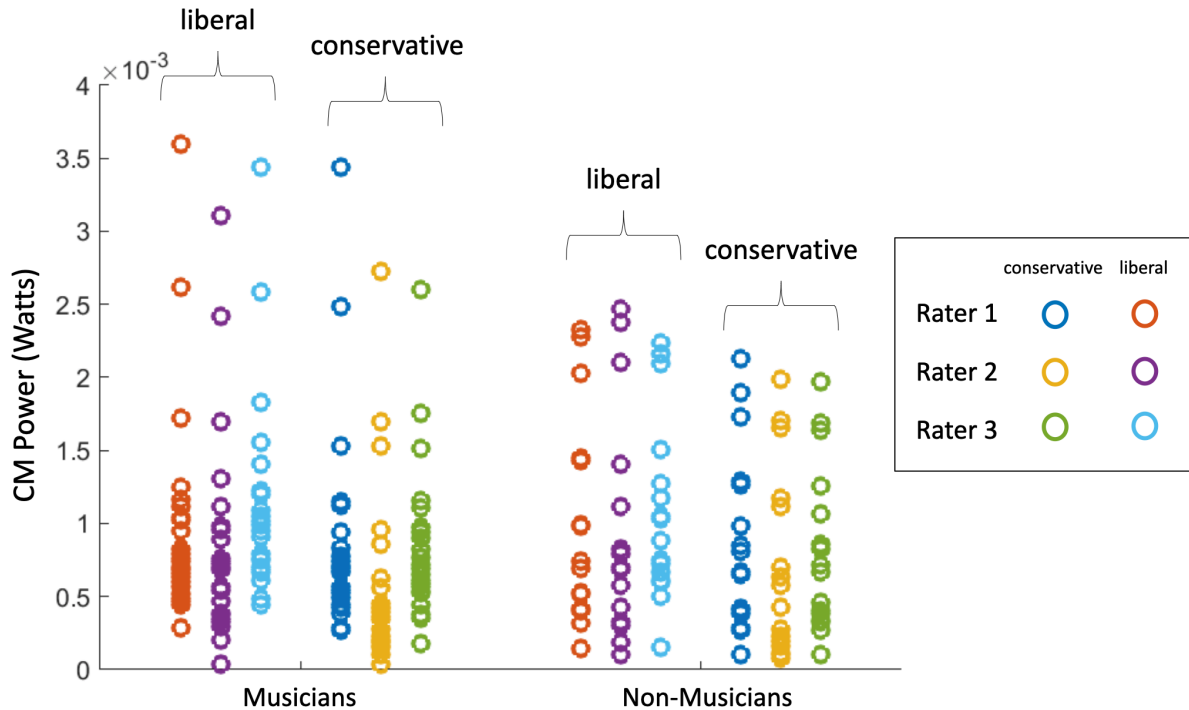


Figure 3.5 Scatterplot of calculated CM power values from each rater between the high-risk musician group and control non-musician group. Measured values under conservative and liberal criteria are shown separately.

Similar to CM/CAP amplitude ratios, the visual distribution of CM power values overlapped within groups among liberal and conservative measures, indicating that amplitude values were judged to be similar between liberal and conservative criteria. The distribution of data points in *Figure 3.5* showed much overlap between groups, with the majority of values in both high-risk and low-risk groups falling below the value of 2. Statistical analyses showed no significant main effect of group on liberal ($F_{1, 39} = 2.301, p = 0.137, \eta_p^2 = 0.056$) or conservative CM power values ($F_{1, 39} = 2.524, p = 0.120, \eta_p^2 = 0.061$). There was no significant interaction between group and rater for liberal criteria ($F_{2, 78} = 1.134, p = 0.327, \eta_p^2 = 0.028, GG = 0.963$),

and a significant main effect of rater on liberal criteria ($F_{2, 78} = 15.725, p = 0.000, \eta_p^2 = 0.287, GG = 0.963$). There was a significant main effect of rater on conservative CM power values ($F_{2, 78} = 19.354, p = 0.000, \eta_p^2 = 0.332, GG = 0.987$), and a significant interaction between group and rater ($F_{2, 78} = 5.359, p = 0.007, \eta_p^2 = 0.3121, GG = 0.987$).

Inter-rater reliability for the CM power measurement was computed using Pearson's r correlations. Under liberal criteria, there was a strong positive correlation that was significant among all raters ($r(41) = 0.966, p = 0.000; r(41) = 0.951, p = 0.000; r(41) = 0.937, p = 0.000$). Likewise under conservative criteria, there was a strong positive correlation that was significant among all raters ($r(41) = 0.926, p = 0.000; r(41) = 0.953, p = 0.000; r(41) = 0.917, p = 0.000$). A table of Pearson's r and p values for inter-rater reliability is shown in *Appendix A.1*.

Chapter 4: Discussion

4.1 Summary of Results

4.1.1 CM Measures

The goal of the current study was to evaluate the utility of the CM as a diagnostic measure for noise-induced CS. Using available ECoHG data from Chang (2020), the results from this study did not find any evidence for significant differences in any measured or calculated CM component between two noise-exposure risk groups; high-risk (music students) and low-risk (controls). Thus, the present study found insufficient evidence to reject the null hypotheses defined in section 1.6, and therefore does not support the idea of using CM amplitude, CM duration, or CM power measures for discriminating between high-risk and low-risk groups.

The non-significant results from CM/CAP amplitude ratio analyses were expected because previous ANSD literature reviewed by Soares et al. (2016) found no significant difference in CM amplitudes from children with ANSD and children with typical hearing. But, because the present study sampled from adult populations, maturational or environmental influences do not appear to change cochlear responses enough to be measured using the methods employed in present study. As shown in *Figures 3.2 to 3.5* in the present study, the high-risk group's results overlapped considerably with the control group. Possible caveats and explanations for the results are detailed in section 4.2.

4.1.1.1 Comparison to Current Literature

As the CM was historically considered to have limited clinical use (Eggermont, 2017b), literature pertaining CM is likewise limited. Click stimuli have been traditionally used in ECoChG to evoke CAP and SP responses (Coats & Dickey, 1970; Picton, 2010). Literature providing large-sample normative CM latency and amplitude data recorded from ET ECoChG exclusively in adults is lacking, particularly in response to click stimuli. One study by Ponton et al. (1992) investigated adult CM responses to masked click stimuli, but did not provide latency or amplitude values.

Literature on normative click-evoked CM data exists for trans-tympanic or surface electrode ECoChG recordings, and from either a wide age range or children exclusively (Arslan, Santarelli, Sparacino, & Sella, 2000; Santarelli et al., 2006; Starr et al., 2001; Hunter et al., 2018). As discussed in section 1.3.4.1, data involving infant and children participants may not be an appropriate to compare to adult data because CM responses, such as absolute amplitude, have been shown to decrease with age (Starr et al., 2001). A possible explanation for this occurrence may be that neural maturation and myelination may strengthen the efferent feedback system. Similarly, CM data recorded from TT and surface electrodes may not provide a proper comparison to data from the present study. CM responses have been shown to decrease with increasing distance between the electrode and the hair cells generating the CM, and thus may require more signal averaging to sufficiently reveal the CM above the noise floor (Ferraro, 2010; Picton, 2010). As such, results from the present study could not be directly compared to current literature involving click-evoked CM responses.

While click-evoked data that includes paediatric ears may not be an appropriate comparison to results from the present study, an informal observation can be made on the

descriptive statistics among CM literature. Differences in age range, testing conditions, and recording parameters among click-evoked CM literature contribute to the variability seen across the data for CM duration and amplitude measures. Select CM duration and amplitude values from relevant ANSD literature are shown in *Appendix A.2*. Among the CM ANSD literature discussed in section 1.3.4.1.1 and listed in *Appendix A.2*, the CM duration data from the present study for the high-risk (mean liberal CM duration across raters: $3.25 \text{ ms} \pm 1.31$ standard deviations to $4.73 \pm 1.25 \text{ ms}$; mean conservative CM duration across raters: $1.75 \pm 0.92 \text{ ms}$ to $2.76 \pm 0.88 \text{ ms}$) and low-risk (mean liberal CM duration across raters: $2.93 \pm 1.25 \text{ ms}$ to $4.82 \pm 1.11 \text{ ms}$; mean conservative CM duration across raters: $1.56 \pm 0.87 \text{ ms}$ to $2.79 \pm 0.75 \text{ ms}$) groups showed some similarity to CM duration data reported for normal participants in Santarelli et al. (2006) (mean CM duration: $4.36 \pm 1.97 \text{ ms}$). This may in part be attributable to researchers including ET-recorded data along with TT-recorded data, and having a participant age range (age range: 7 months to 47 years) that overlapped with the age group recruited for the present study (age range: 18-28 years). The mean CM duration reported for the ANSD group in Santarelli et al. (2006) was higher than the presents results, although large variance in CM duration within the ANSD group was reported (mean CM duration: $6.77 \pm 2.58 \text{ ms}$). Santarelli and colleagues (2006) found evidence for a significant difference in CM duration between ANSD and normal groups—this may have been influenced by the severity of hearing deficits experienced by those in their ANSD group that is not seen in participants of either group in the present study. Participant effects on the CM are further discussed in section 4.2.

4.1.2 Lifetime Noise Exposure

The present study found no significant effect of group on lifetime noise exposure quantified by using NESI, even after exclusion of outliers. However, the results trended toward significance and would have been significant if an uncorrected p-value <0.05 was used. No relationship was found among NESI scores and CM duration, CM/CAP amplitude ratio, CM power, or raters. These results may indicate that 1) there is not a large enough difference in lifetime noise exposure between groups, 2) the sample size was not large enough to reach a significant difference in noise exposure between groups, or 3) NESI is not a reliable predictor for a difference in noise exposure between groups in the context of CS. These are further discussed in sections 4.2.3 to 4.2.5.

4.1.3 Raters

A significant effect of rater was found in liberal and conservatively measured CM duration values and computed CM power values. Differences between raters demonstrate the subjectivity in visual identification and labelling of CM latency, despite an attempt to offset variability through liberal and conservative criteria. Variance in rater experience and expertise may be a possible reason for the present results. In addition, there was no significant effect of rater on liberal CM/CAP amplitude ratio, but a significant effect rater was found in the conservative condition. Uniformity among raters was expected because they were directed to identify the largest peak-to-peak amplitude, which were prominently visible above the noise floor within the first couple of milliseconds. CM/CAP amplitude ratios should thus not be influenced much by the decision of when to place the marker for CM duration, which was much

more variable. However, subjective variability the marking process is inherent, and so the results indicate that clinician variability in peak marking can be expected.

4.2 Possible Explanations for Current Findings

4.2.1 ECochG Stimuli and Recording Parameters

The present study was a retrospective analysis on data originally collected to evaluate the efficacy of ECochG-derived SP/CAP ratios in the diagnosis of noise-induced CS. As such, the stimulus and recording parameters were optimized to elicit these neural responses in the waveform. Clinically, ET ECochG tests are typically used to record the SP/CAP response ratio, whereas the CM is not often evaluated clinically. This may be due to the CM being susceptible to low response reliability and artifact contamination (Noguchi, Nishida, & Komatsuzaki, 1999; Yoshie & Yamaura, 1969). Sohmer & Feinmesser (1967) noted that click-evoked CMs recorded from ET ECochG are too small and inefficient for clinical or research utility. Conventionally, tone stimuli have been favoured over click stimuli to elicit the CM as the magnitude of the response is larger—especially in lower frequencies (Eberling & Salomon, 1973; Noguchi, Nishida, & Komatsuzaki, 1999; Zhang, 2012). Click-evoked CMs have been shown to have shorter oscillating cycles than tone-evoked CMs (Zhang, 2012). Several factors may be involved in the decreasing response magnitude including tonotopic frequency mapping, changing stiffness and width, and OHC density along the basilar membrane. Ponton, Don, & Eggermont (1992) showed, using ET-recorded high-pass noise masked click stimuli, that CM latency increased when the derived band center-frequency was lower, indicating that lower frequency stimuli could provide larger CM responses above SNR. However, click stimuli with a high concentration of

energy in the high-frequency region mainly excite the basal turn of the cochlea (Sohmer & Pratt, 1976).

As the broadband click stimulus used in the present study has a substantial high-frequency component, the magnitude of the CMs may have been compromised due to stimulus parameters. This may provide a possible reason for the lack of ECoChG measure differences between groups, but this is not conclusive from the current findings. Noise-induced hearing loss often begins in the basal cochlear region, with professional musicians showing losses in frequencies ≥ 3 kHz first (Di Stadio et al., 2018). A paradoxical complication in using CMs to identify individuals at high risk of having a HHL is that hearing losses usually start to occur in the high-frequencies (the basal cochlear regions), however the CMs from the high-frequency basal regions are smaller and more difficult to record via ET ECoChG. Thus, a potential caveat to the present study's findings is that there might have been insufficient sensitivity using the CM to identify high-risk individuals.

Electrode distance from the hair cells also influence the sensitivity of the recordings. TT has been shown to produce much larger CM amplitudes compared to ET, and both methods yield larger amplitudes than surface electrodes due to the distance from the generators (Picton, 2010; Schoonhoven, Fabius, & Grote, 1995). The absolute amplitudes recorded by ET electrodes could be affected by placement (Ferraro, 2010). Consultation with the original researcher of the present data revealed that the data were not always recorded with the electrode on the TM, but sometimes approximate to the TM due to participant discomfort. Thus, the raw amplitude data in the present study show some variances. The variance was normalized across participants by factoring in the CAP amplitude, which can also be altered by electrode distance from the

cochlea. However, due to the nature of ET electrodes being at a distance from the cochlea— an average 2.5 mm between the tympanic membrane and the promontory (Beck, 1970)—the CM is subject to attenuation. Thus, a possible explanation for the lack of difference in CM duration between groups could be that the hypothesized prolonged cycles of the CM in the high-risk group may have been buried within the background EEG noise and gone unnoticed by the raters. In comparison, TT recordings are closer to the cochlea, which in turn reduces possible artifacts. This results in considerably larger amplitudes, and may allow the trailing end of the CM to be large enough above the background noise to be visually identified by raters. It is interesting to note, however, that some studies have shown the latencies of ET- and TT-recorded CMs were similar (Schoonhoven, Fabius, & Grote, 1995; Noguchi, Nishida, & Komatsuzaki, 1999).

In some of the participant data, the RC-CC and CC-RC waveforms appeared to contain neural components in the tracings. An example of this presentation is shown in *Figure 4.1*. Similar findings were reported in Ponton, Don, & Eggermont (1992), who found some click-evoked CMs with neural components embedded. They postulated that the low-frequency contributions of the click stimuli resulted in phase-locking, which may have prevented the complete removal of all neural responses (i.e. waves I-V) through subtraction of the waveforms. The presence of neural components was later demonstrated in CMs recorded from low-frequency stimuli by Kameron et al. (2016). The presence of neural components can affect the interpretation of CM latency. Visual identification of CM latency in these situations depended on the raters' subjective decision as to what aspects of the waveform was a CM, a neural response, or an artifact. This difficulty may have partially contributed to the statistical variances seen between raters.

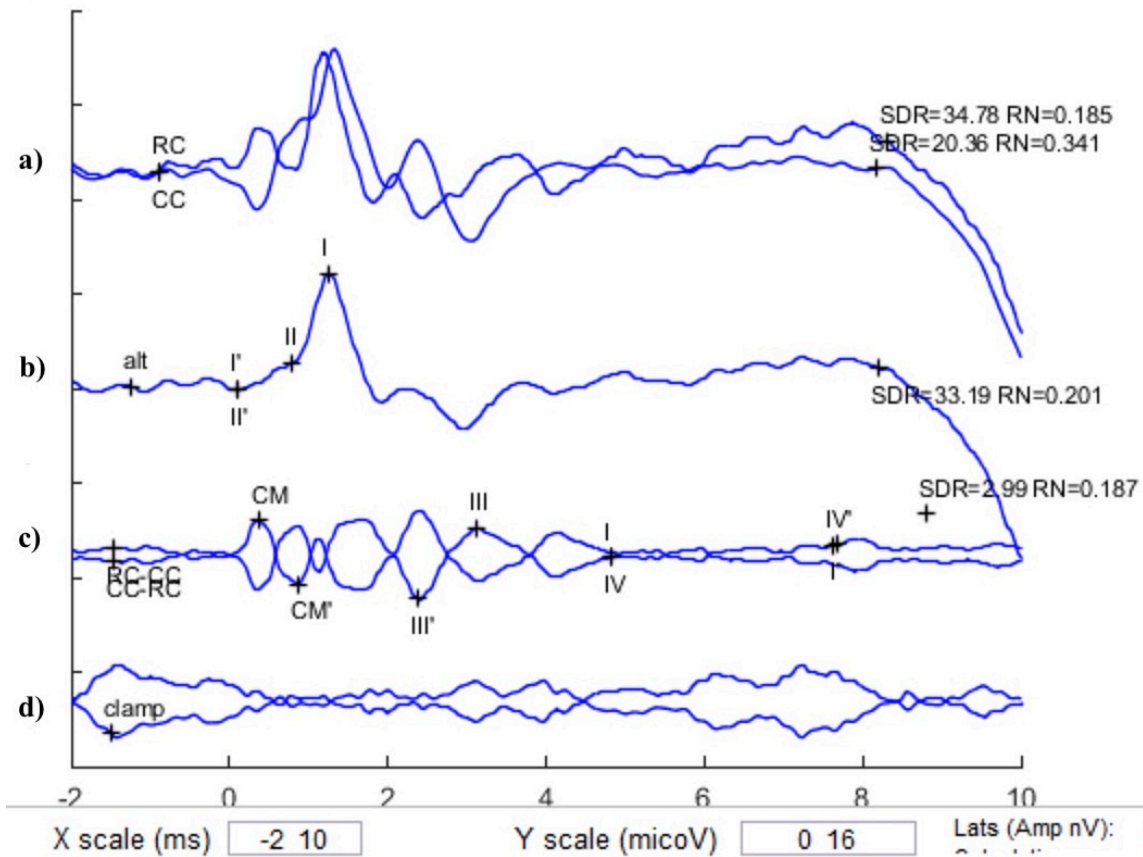


Figure 4.1 ECoG recordings from a high-risk participant with possible neural components within subtracted CM-only tracings (RC-CC/2). Obtained from sABR v10.3. Averages are sweeps-weighted, while subtractions are amplitude-weighted. *a*) Averaged RC and CC waveforms recorded in response to 11.3 Hz click stimuli, overlaid to display phase-inverted CM oscillations. *b*) Alternating waveform response to 11.3 Hz stimuli with the CM eliminated to show non-inverting neural components. AP and SP amplitudes labelled I-I' and II-II', respectively. *c*) Difference waveform RC-CC achieved by subtracting the averaged CC from the averaged RC waveform and multiplying by 0.5. CC-RC waveform achieved by multiplying the RC-CC waveform by -1. Non-inverting neural components have been eliminated from both overlaid tracings to show the CM. Responses to 11.3 Hz stimuli. Conservative and liberal estimates of CM duration labelled III and IV. Peak-to-trough CM amplitude labelled CM-CM'. *d*) Clamped-tube tracings with the CM and non-inverting neural components eliminated. Inverted clamped-tube tracing achieved by multiplying the recording by -1.

4.2.2 Sensitivity of the CM to CS in Humans

The CM is a measure of hair cell bioelectric activity, and thus is a response reflecting the function of hair cells and not postsynaptic ANFs. With accumulating evidence on CS suggesting degradation of the synapse involving presynaptic ribbons and postsynaptic ANFs, the results of the present study may provide evidence that noise-induced CS cannot be assessed via the integrity of the hair cell—perhaps because the pathology lies at the level of the synapse and not before it. In the present study, the CM was investigated because of the potential effects CS may have on the efferent braking feedback system (see section 1.2.1.1 for review). If CS reduces ANF communication, then the subsequent efferent circuitry may also be reduced, resulting in a “runaway” feed-forward system that continually perpetuates cochlear non-linearity via OHC activation.

The lack of significant differences in CM measures between groups may suggest that either ET ECoG or the CM—or perhaps neither measure—are sensitive enough for CS identification. The CM is often used in the differential diagnosis of ANSD as an adjunct measure of hair cell function when OAEs are absent. However, it should be noted that the reported functional consequences of genetic and congenital ANSD are often more severe than the reported consequences of HHL individuals with high lifetime noise exposure and normal audiometric thresholds (Moser & Starr, 2016; Rance & Starr, 2015). Many children with ANSD will opt for cochlear implantation due to poor speech perception (Harrison et al., 2015; Teagle et al., 2010; Sarankumar et al., 2018; Shaikh, Eldin, & Abusetta, 2016). With CS, it has been suggested that the perceptual consequences in humans may be too diffuse or inconsequential to detect via electrophysiological and behavioural measures (Grose, Buss, & Hall III, 2017). Consequently, if

there is any effect the CS may have on the efferent feedback system, it may also be too diffuse or inconsequential to detect using an indirect ECoChG measure. It should also be noted that ECoChG findings are between ANSD cases of auditory neuropathy and auditory synaptopathy, such as patients with OPA1-associated auditory neuropathy and OTOF-associated auditory synaptopathy, are often very similar (Moser & Starr, 2015). This indicates that ECoChG, and the CM, may not be precise enough to identify what pathology exists, only that a pathology may be present when large enough. It may further point to the relative insensitivity of the CM in differentially diagnosing CS from other auditory dysfunctions (e.g. auditory neuropathy, central auditory processing disorder), even if all testing parameters and conditions were optimized. In the context of CS, it is particularly difficult to conclude whether the ECoChG-evoked CM is an insensitive measure, or if CS is not substantial in humans, because of a lack the lack of literature on the topic. In the landscape of human CS research, inconsistent test parameters used among research groups make it difficult to compare and draw conclusions (Bramhall et al., 2019).

4.2.3 Effects of Age

Evaluating the effect of CS on the CM for the young adult population has inherent associated difficulties. Recordings of the CM are seemingly affected by the degree of hearing loss in the audiogram in both children and adults (Starr et al., 2001; Yoshie & Yamaura, 2009), and children with ANSD have been shown to have prolonged CM durations and larger peak CM amplitudes (Smith, 2018; Santarelli et al., 2006). Current literature comparing the CM of normal hearing and ANSD patients often include paediatric data. When considering the lack of difference in CM found between groups in the present study, it is interesting to note that while

Starr et al. (2001) found a difference in CM amplitudes between groups with and without ANSD under 10 years of age, participants above the age of 10 (age range: 11-50) did not show significant differences. In the present study—which likewise showed no evidence for significant differences in CM amplitudes between noise-exposure groups—the participant age range was between 18-28.

Alternatively, the opposite case can be made. The young age of recruited participants may be a possible explanation for the lack of differences. Young music students may not endure significant noise-induced hearing loss so early in their careers. Seminal studies by Kujawa and Liberman on CS revealed substantial but delayed cochlear nerve degeneration in mice models 2 years postnatal age, and minimal degeneration with virtually no hair cell loss when observed shortly after early-age noise exposure (Kujawa & Liberman, 2006; Kujawa & Liberman, 2009). Two years of aging in mice roughly equates to 60 human years of aging. As participants in the present study ranged between 18-28 years of age, it is possible that significant ANF and hair cell degeneration may not yet be exhibited in the participants until later in life. Couth et al. (2020) suggested that CS in humans may be more related to the aging auditory system than noise exposure. In humans, MOC density (Liberman & Liberman, 2019) and synaptic count (Makary et al., 2011; Viana et al., 2015) have been shown to decrease significantly with age. Loss of hair cell-ANF synapses accumulates steadily—reaching about 25% at middle age—long before any significant hair cell loss is observed (Sergeyenko, Lall, Liberman, & Kujawa, 2013). In the Liberman et al. (2016) HHL ECochG study, a significant difference was found in the SP/CAP ratios between musicians and non-musicians. The participant age range was 18-41, compared to the participant age range (18-28) in the present study. Because older adults may have higher

MOC density or cochlear synaptic losses (Liberman & Liberman, 2019; Makary et al., 2011; Viana et al., 2015), the older participants in their high-risk sample may have had more detectable effects of CS on their hearing system than the musician group in the present study. Inclusion of older participants in the present may resulted in different enough SP/CAP ratios between groups.

4.2.4 Recruitment and Sample Size

Recruitment criteria may have an a priori effect on the CM data. As mentioned in the above section, the significant results found in Liberman et al. (2016) may have been in part due to the difference in recruitment compared to the present study. The study Liberman et al. (2016) utilized a more lenient participant inclusion criteria and less precise lifetime noise exposure questionnaire. By comparison, Prendergast et al., (2017a)—who implemented a more stringent inclusion criteria along with a cumulative noise exposure questionnaire similar to the NESI—found no evidence for a difference between groups in the SP/CAP ratio using a similar ECochG protocol to the present study. Significant differences between high-risk and low-risk groups could not be replicated using mastoid (Prendergast et al. , 2018) or ET ECochG (Chang, 2020) when following a strict recruitment process and thorough questionnaire. The high-risk group in the present study reported no perceptual listening difficulties, whereas Plack et al. (2014) noted that a characteristic of HHL was higher incidences of listening difficulty in noise. As such, the sample population in the high-risk group of the present study may have had insufficient CS on their hearing system to be detectable using ET ECochG.

Another possible explanation may be that the present study did not have a large enough sample size. Sample size was small and uneven between groups, as well as gender. As shown in

section 3.1, NESI scores reached near significance for a difference between groups. If a Bonferroni correction was not applied, there would have been evidence that the musician's NESI scores were higher than the non-musician NESI scores. Monette (2020), part of the present study's larger collaborative HHL project, found evidence for a significant difference in NESI scores between musicians and nonmusicians in a larger sample. These different findings indicate that present study was most likely underpowered due to sample size and thus unable to detect any recordable differences in CM characteristics between the music students and controls.

4.2.5 Noise Exposure and Reliability of NESI

Another possible explanation for the lack of difference in electrophysiological measures between groups may be that the young university music students do not represent a population with enough accumulated neural degeneration through significant noise exposure. The cumulative lifetime noise exposure may have been too similar for music students and non-musicians, despite music students practicing with instruments daily. The risk of hearing impairment increases by age from cumulative noise exposure throughout musicians' careers, with the risk increasing 26% over 40 years of professional playing (Pawlaczyk-Łuszczynska, Dudarewicz, Zamojska, & Śliwinska-Kowalska, 2011). Indeed, many of the noise exposure studies discussed in section 1.4 often involve professional musicians well into their careers. As lifetime noise exposure is cumulative over time, and participants are in the early stages of their musical careers, it is unsurprising that the high-risk group had unsubstantial raw NESI scores.

Alternatively, the measure used to quantify lifetime noise exposure in this study did not faithfully represent the true noise exposure experienced by participants. As mentioned in section

3.1, three raw NESI scores excluded from analysis. The three scores were much higher compared to the raw scores of other individuals, and given that one NESI unit equated to one working year of 90 dBA noise exposure, the extreme scores were impractical. These NESI scores may be an indication of the unreliability of a self-report interview format. The NESI format estimates noise levels by asking individuals their believed level of vocal effort if they spoke to a conversation partner during each reported noisy activities. This qualitative effort level is then converted to a quantitative dBA, with possible values ranging from 80-110 dBA in the NESI table (see Guest et al. (2018) Supplementary Material 2 for review). The unusually high scores may have resulted from erroneous participant interpretation of loudness for each noisy activity. In regards to the three outlier NESI scores recorded, participants differentially reported subjective vocal effort to similar activities—such as solo practicing, orchestral practice, and going to noisy entertainment establishments. The discrepancies resulted in some participants scoring low despite countless hours of instrument practice, and others reporting NESI scores above 100.

It may be entirely possible that the variance in estimated noise exposure is related to the differences in output sound level between instruments. The exact noise level musicians are exposed to depends on instrument choice and ear lateralization (Berger et al., 2006; O'Brien, Driscoll, & Ackermann, 2013; Schmidt et al., 2014; Qian et al., 2011). Rehearsals can range between 77-98 dBA depending on the type of music played (Berger et al., 2006). It may also be possible that orchestral practice may not be dangerously loud enough to cause harm for young music students. Despite some studies suggesting musicians exceed daily noise limit, Behar et al. (2018) measured an average 85 dBA exposure level during performance with the National Ballet of Canada Orchestra—the accepted daily occupational noise limit for an 8-hour shift is 85 dBA

per National Institute for Occupational Safety and Health (Centers For Disease Control and Prevention, 2018). However, the NESI level estimation is ultimately subjective and variable—as evidenced by both the outliers and the lack of difference between normal, healthy participants and music students with extensive noise exposure.

4.2.6 Human Susceptibility to CS

Recent evidence suggests that primates may be more resilient to cochlear damage than rodents (Valero et al., 2017). As such, rodent models for CS may not be fully representative or generalizable to human CS and its perceptual consequences. In the seminal study by Kuwaja & Liberman (2009) conducted on mice, researchers applied a 100 dB SPL noise for 2 hours. When correcting for audiometric differences between species, Dobie & Humes (2017) deduced that this noise exposure would well exceed the recommended daily noise dose in humans. They suggested that a 114 dB SPL level of noise continuously presented for 2 hours would be the equivalent level of exposure for humans to experience similar results of CS—a level of sound energy that would be very unlikely in the day-to-day experience. This raises the question of whether noise-induced CS is prevalent among humans. Human postmortem temporal bone studies suggest that loss of cochlear synapses in the absence of hair cell damage does occur, but that its presence may be age-dependent (Makary et al., 2011; Viana et al., 2015). Indeed, results from the present study, along with conflicting evidence from various human electrophysiological studies on CS (see section 1.3 for review), may suggest that the perceptual consequences of CS are too diffuse or inconsequential to detect. Furthermore, Couth et al. (2020) surmised that adults—particularly young adults such as those recruited for the present study—may be more resilient to CS. Thus,

any effect of CS on the human efferent feedback system may not be large enough to detect via the ET ECoG-evoked CM, especially in among the age group recruited in the present study.

4.3 Study Limitations

The present study suffered from both a low sample size and an uneven number of participants in between groups (high-risk: $n = 27$; control: $n = 14$), which may have contributed to the insignificant results. The high-risk group comprised of 16 subjects while only 8 subjects were included in the control group. Should the present study have recruited more subjects, the distribution of NESI scores within the high-risk group could have been interpreted more confidently. However, the clinical viability of testing should show high levels of discriminability between groups, which appears unlikely to occur for the noise-exposure risk groups recruited in this study because of such a large overlap in the outcome distributions between the groups.

Another limitation to the present study was the difference in CM labelling experience and skill between raters, resulting in significant differences in multiple measured CM properties between raters. The wide range of raters' experience in visual waveform identification—which varied from novice to expert CM—may have introduced variability into the data. This highlights the subjectiveness in using the CM for CS diagnosis or screening. Waveform labelling often requires making decisions on, and parsing of the waveforms can be particularly difficult with more waveforms, as shown above in *Figure 4.1*. Future studies should aim to control for inter-rater variability through sufficient CM labelling practice, or vet raters with a baseline level of experience on visual CM identification.

Another confounding variable may have been introduced through placement of the ET electrode. During the ECochG procedure, verification of electrode contact on the tympanic membrane relied on a combination subjects reporting when they've heard a 'thump', low electrode impedance, and otoscopy. Despite this, variance in the distance between the electrode tip and the tympanic membrane surface may have persisted. As Ferraro (2010) noted, this placement technique is conducted partially 'blind' due to the electrode obscuring view of the tympanic membrane. The researcher of the original study, from which the present data were collected, could not guarantee the placement of the electrode on the tympanic membrane. Some subjects reported discomfort during insertion of the electrode in the auditory canal, prompting the researcher to minimize further movement of the electrode.

To help eliminate artifact and lower background noise, TT ECochG—in which an electrode is placed on the promontory of the middle ear—would provide cleaner recordings (Ferraro, 2010). However, researchers would face other limitations—invasiveness of a procedure to insert the needle electrode, and the requirement for a physician to perform the surgical insertion. In addition, clinical audiologists would need to refer patients to otolaryngologists which would limit the viability of using CMs as a diagnostic measure within standard audiological practice.

Many subjects from the present study were tested in a non-shielded room before researchers moved to a shielded, soundproof testing booth. This change was in response to unresolvable stimulus artifacts, likely from electromagnetic radiation of an external source, introduced to recordings. Improper shielding has been shown to significantly affect ECochG recordings (Simpson, Jennings, & Margolis, 2020). Thus, it is possible that location changes may

have added some variability to recordings, where some subject data were easier to label than others.

4.4 Future Research Directions

The effects of individuals at high-risk of noise-induced CS is yet to be fully understood, and the diagnostic tools are either primitive or unreliable for identifying individuals with CS. Further ECoChG investigation will provide insight to this less-understood subfield of audiology. A follow-up to the present study will benefit from an original protocol tailored to specifically evoke a prominent CM response. While the present study focused on click-evoked CM responses, tone stimuli paired with proper, consistent electrical shielding will help separate the CM from artifact (Riazi & Ferraro, 2008). Tone stimuli will allow the researcher to more specifically target areas of the cochlea susceptible to noise-induced CS. Additionally, simultaneous ABR recording via a mixed ABR-ECoChG montage may be useful to compare the efficacy of either test in the diagnosis of CS in humans.

Further research on the effects of CS on the CM should aim to recruit participants from a larger age range—preferably from a population with more long-term cumulative noise exposure. Recruitment of professional musicians with a minimum requirement of performance experience yet high risk of noise exposure would be warranted. Given that it may be difficult recruit older individuals with a history of noise exposure and no audiometric threshold shifts, it may be beneficial to extend the research to those with tinnitus and normal audiograms. CS of low spontaneous-rate ANFs have been proposed to underlie the development of chronic tinnitus (Schaette & McAlpine, 2011). There is a higher prevalence of tinnitus in older adults, and cases

of tinnitus with normal audiograms are often reported in individuals with cumulative leisure-time noise exposure (Shargorodsky, Curhan, & Farwell, 2010). Guest et al. (2017) investigated whether individuals with tinnitus and normal audiograms may have ABR responses indicative of CS, with results revealed to be unpromising. However, no relevant studies have been conducted with ECoChG.

It may also be beneficial to recruit participants whom report perceptual difficulties such as degraded speech in noise with no elevated hearing thresholds. Noise-induced CS has been shown to occur primarily in high-threshold ANFs that respond to supra-threshold sound stimuli, which can result in normal hearing thresholds paired with diminished supra-threshold hearing abilities (Furman, Kujawa, & Liberman, 2013; Bharadwaj et al., 2014). Plack et al. (2014) noted that a characteristic of HHL involved individuals with more noise exposure reporting higher incidences of listening difficulty in noise. Inclusion of these populations may provide more promising ECoChG results.

Studies have provided differing results for and against noise-induced CS, which may be attributable to the varying protocols across research groups in the field (Bramhall et al., 2019). This pattern extends to the quantification of cumulative noise exposure in humans. Researchers have a history of employing noise exposure questionnaires that varied across studies (Carter, Black, Bundy, & Williams, 2016; Dalton et al., 2001; Jokitulppo, Toivonen, & Björk, 2006; Keppler, Dhooge, & Vinck, 2015; Liberman et al., 2016; Prendergast et al., 2017b; Stamper & Johnson, 2015a/b). Perhaps it may be beneficial to employ an alternative noise exposure history questionnaire that has been used by other research groups to maintain consistency across results. If continuing to use NESI, future studies may find it beneficial to incorporate examples of vocal

effort and approximate sound levels for particular activities, in an effort to more accurately capture noise exposure history. Providing examples to participants may help eliminate some of the NESI score variability seen in the present study. For future studies involving musicians, additional data collection on instrument type and ear lateralization may help to better account for the inherent variability of noise exposure through musical performance.

Finally, while the present study focused on noise-induced CS, research involving other etiologies of CS may be more compatible for the investigation ECoChG diagnostic utility. Auditory synaptopathy resulting from congenital ototoxicity may be a potential target population for CS research (Moser & Starr, 2016). Liberman, Liberman, & Maison (2015) showed that in mice suffering conductive hearing losses, such as chronic otitis media or missing tympanic membranes, CS was also observed. Similarly, Cho et al. (2013) showed that blast-exposed mice showed patterns of CS in the apical cochlea tuned to low frequencies. These results suggest that blast exposure or TBI in humans may lead to CS. As ECoChG-recorded CMs are optimally elicited using low-frequency stimuli, CS research involving TBI patients may be promising.

Chapter 5: Conclusion

The present study investigated the effect of CS on the CM using ET ECoChG. The results of our study showed no relationship among lifetime noise exposure and CM duration, CM/CAP amplitude, or CM power. Particularly, there were no observable differences in the electrophysiology between the high-risk and control group. The outcomes suggest that ET ECoChG is an insensitive diagnostic tool for noise-induced CS in humans within the populations sampled in this study. The results presented here do not definitely determine the efficacy of either ECoChG or CM as diagnostic measures for CS—a broader investigation is needed. While inconclusive, the present study may add to the larger landscape of CS research. Further CS research may provide more insight to the development of a sensitive diagnostic battery that could render the “hidden” portion of the term “HHL” obsolete.

Bibliography

- Andreollo, N. A., Santos, E. F., Araújo, M. R., & Lopes, L. R. (2012). Rat's age versus human's age: what is the relationship?. *Brazilian Archives of Digestive Surgery*, 25(1), 49–51.
- Arslan, E., Santarelli, R., Sparacino, G., & Sella, G. (2000). Compound action potential and cochlear microphonic extracted from electrocochleographic responses to condensation or rarefaction clicks. *Acta Oto-Laryngologica*, 120(2), 192–196.
- Beck, C. (1970). Anatomy of the ear. In *Otorhinolaryngology* (pp. 1–49). New York: Georg.
- Behar, A., Chasin, M., Mosher, S., Abdoli-Eramaki, M., & Russo, F. A. (2018). Noise exposure and hearing loss in classical orchestra musicians: A five-year follow-up. *Noise & Health*, 20(93), 42–46.
- Berger, E. H., Neitzel, R., & Kladden, C. A. (2006). Noise navigator sound level database with over 1700 measurement values. University of Washington, Department of Environmental & Occupational Health Sciences, Seattle. Retrieved from <https://multimedia.3m.com/mws/media/888553O/noise-navigator-sound-level-hearing-protection-database.pdf>.
- Berlin, C. I., Hood, L. J., Morlet, T., Wilensky, D., Li, L., Mattingly, K. R., Taylor-Jeanfreau, J., Keats, B. J., John, P. S., Montgomery, E., Shallop, J. K., Russell, B. A., & Frisch, S. A. (2010). Multi-site diagnosis and management of 260 patients with auditory neuropathy/dys-synchrony (auditory neuropathy spectrum disorder). *International Journal of Audiology*, 49(1), 30–43.

- Bharadwaj, H. M., Mai, A. R., Simpson, J. M., Choi, I., Heinz, M. G., & Shinn-Cunningham, B. G. (2019). Non-invasive assays of cochlear synaptopathy - candidates and considerations. *Neuroscience*, *407*, 53–66.
- Bharadwaj, H. M., Masud, S., Mehraei, G., Verhulst, S., & Shinn-Cunningham, B. G. (2015). Individual differences reveal correlates of hidden hearing deficits. *The Journal of Neuroscience*, *35*(5), 2161–2172.
- Bharadwaj, H. M., Verhulst, S., Shaheen, L., Liberman, M. C., & Shinn-Cunningham, B. G. (2014). Cochlear neuropathy and the coding of supra-threshold sound. *Frontiers in systems Neuroscience*, *8*, 26.
- Borg, E., Canlon, B., & Engström, B. (1995). Noise-induced hearing loss. Literature review and experiments in rabbits. Morphological and electrophysiological features, exposure parameters and temporal factors, variability and interactions. *Scandinavian Audiology Supplementum*, *40*, 1–147.
- Bourien, J., Tang, Y., Batrel, C., Huet, A., Lenoir, M., Ladrech, S., ... & Wang, J. (2014). Contribution of auditory nerve fibers to compound action potential of the auditory nerve. *Journal of Neurophysiology*, *112*(5), 1025–1039.
- Bramhall, N., Beach, E. F., Epp, B., Le Prell, C. G., Lopez-Poveda, E. A., Plack, C. J., Schaette, R., Verhulst, S., & Canlon, B. (2019). The search for noise-induced cochlear synaptopathy in humans: Mission impossible?. *Hearing Research*, *377*, 88–103.
- Bramhall, N. F., Konrad-Martin, D., McMillan, G. P., & Griest, S. E. (2017). Auditory brainstem response altered in humans with noise exposure despite normal outer hair cell function. *Ear and Hearing*, *38*(1), e1–e12.

- Carter, L., Black, D., Bundy, A., & Williams, W. (2016). An estimation of the whole-of-life noise exposure of adolescent and young adult Australians with hearing impairment. *Journal of the American Academy of Audiology*, 27(9), 750–763.
- Centers For Disease Control and Prevention. (2018). *Hearing and noise prevention*. Retrieved from <https://www.cdc.gov/niosh/topics/noise/>.
- Chambers, A. R., Resnik, J., Yuan, Y., Whitton, J. P., Edge, A. S., Liberman, M. C., & Polley, D. B. (2016). Central gain restores auditory processing following near-complete cochlear denervation. *Neuron*, 89(4), 867–879.
- Chang, C. (2020). Electrocochleography as a diagnostic tool for noise-induced cochlear synaptopathy. *The University of British Columbia*. Retrieved from <http://hdl.handle.net/2429/74289>.
- Chasin, M. (2009). Hearing loss prevention for musicians and introduction to the problem. *Hearing loss in musicians: Prevention and management*. San Diego: Plural Publishing, 1–10.
- Chesky, K. (2010). Measurement and prediction of sound exposure levels by university wind bands. *Medical Problems of Performing Artists*, 25(1), 29–34.
- Cho, S. I., Gao, S. S., Xia, A., Wang, R., Salles, F. T., Raphael, P. D., ... & Rasband, M. N. (2013). Mechanisms of hearing loss after blast injury to the ear. *PloS one*, 8(7).
- Coats, A. C. & Dickey, J. R. (1970). Nonsurgical recording of human auditory nerve action potentials and cochlear microphonics. *Annals of Otology, Rhinology & Laryngology*, 79(4). 844–52.

- Costalupes, J.A. (1985). Representation of tones in noise in the responses of auditory nerve fibers in cats. I. Comparison with detection thresholds. *The Journal of Neuroscience*, *5*, 3261–3269.
- Couth, S., Prendergast, G., Guest, H., Munro, K. J., Moore, D. R., Plack, C. J., Ginsborg, J., & Dawes, P. (2020). Investigating the effects of noise exposure on self-report, behavioral and electrophysiological indices of hearing damage in musicians with normal audiometric thresholds. *Hearing Research*, *395*, 108021.
- Dallos, P., & Cheatham, M. A. (1976). Production of cochlear potentials by inner and out hair cells. *The Journal of the Acoustical Society of America*, *60*, 510–512.
- Dallos, P. (1983). Some electrical circuit properties of the organ of Corti. I. Analysis without reactive elements. *Hearing Research*, *12*, 89–120.
- Dalton, D. S., Cruickshanks, K. J., Wiley, T. L., Klein, B. E., Klein, R., & Tweed, T. S. (2001). Association of leisure-time noise exposure and hearing loss. *Audiology : Official Organ of the International Society of Audiology*, *40*(1), 1–9.
- Davis, R. I., Ahroon, W. A., & Hamernik, R. P. (1989). The relation among hearing loss, sensory cell loss and tuning characteristics in the chinchilla. *Hearing Research*, *41*(1), 1–14.
- Darrow, K. N., Maison, S. F., & Liberman, M. C. (2007). Selective removal of lateral olivocochlear efferents increases vulnerability to acute acoustic injury. *Journal of Neurophysiology*, *97*(2), 1775–1785.
- Deltenre, P., Mansbach, A. L., Bozet, C., Clercx, A., & Hecox, K. E. (1997). Auditory neuropathy: A report on three cases with early onsets and major neonatal illnesses. *Electroencephalography and Clinical Neurophysiology*, *104*(1), 17–22.

- Di Stadio, A., Dipietro, L., Ricci, G., Della Volpe, A., Minni, A., Greco, A., de Vincentiis, M., & Ralli, M. (2018). Hearing loss, tinnitus, hyperacusis, and diplacusis in professional musicians: A systematic review. *International Journal of Environmental Research and Public Health*, 15(10), 2120.
- Dobie, R. A., & Humes, L. E. (2017). Commentary on the regulatory implications of noise-induced cochlear neuropathy. *International Journal of Audiology*, 56, 74–78.
- Dudarewicz, A., Pawlaczyk-Łuszczynska, M., Zamojska-Daniszewska, M., & Zaborowski, K. (2015). Exposure to excessive sounds during orchestra rehearsals and temporary hearing changes in hearing among musicians. *Medycyna Pracy*, 66(4), 479–486.
- Eggermont, J. J. (1976). Electrocochleography. In: W. D. Keidel & W. D. Neff (Eds.), *Handbook of Sensory Physiology* (pp. 625–705). Berlin: Auditory system, Springer Verlag.
- Eggermont, J. J. (2017). Chapter 1 - Hearing Basics. In J. J. Eggermont (Ed.), *Hearing Loss* (pp. 3–36). Academic Press.
- Eggermont, J. J. (2017). Ups and downs in 75 years of electrocochleography. *Frontiers in Systems Neuroscience*, 11(2), 1–21.
- Elberling, C., & Salomon, G. (1973). Cochlear microphonics recorded from the ear canal in man. *Acta Oto-Laryngologica*, 75(2-6), 489–495.
- Fettiplace R. (2017). Hair cell transduction, tuning, and synaptic transmission in the mammalian cochlea. *Comprehensive Physiology*, 7(4), 1197–1227.
- Fernandez, K. A., Jeffers, P. W., Lall, K., Liberman, M. C., & Kujawa, S. G. (2015). Aging after noise exposure: Acceleration of cochlear synaptopathy in "recovered" ears. *The Journal of Neuroscience*, 35(19), 7509–7520.

- Fernandez, K. A., Guo, D., Micucci, S., De Gruttola, V., Liberman, M. C., & Kujawa, S. G. (2020). Noise-induced cochlear synaptopathy with and without sensory cell loss. *Neuroscience*, *427*, 43–57.
- Ferraro, J. A. (2010). Electrocochleography: A review of recording approaches, clinical applications, and new findings in adults and children. *Journal of the American Academy of Audiology*, *21*(3), 145–152.
- Furman, A. C., Kujawa, S. G., & Liberman, M. C. (2013). Noise-induced cochlear neuropathy is selective for fibers with low spontaneous rates. *Journal of Neurophysiology*, *110*(3), 577–586.
- Glueckert, R., Bitsche, M., Miller, J. M., Zhu, Y., Prieskorn, D. M., Altschuler, R. A., & Schrott-Fischer, A. (2008). Deafferentation-associated changes in afferent and efferent processes in the guinea pig cochlea and afferent regeneration with chronic intrascalar brain-derived neurotrophic factor and acidic fibroblast growth factor. *The Journal of Comparative Neurology*, *507*(4), 1602–1621.
- Gopal, K. V., Chesky, K., Beschoner, E. A., Nelson, P. D., & Stewart, B. J. (2013). Auditory risk assessment of college music students in jazz band-based instructional activity. *Noise & Health*, *15*(65), 246–252.
- Grose, J. H., Buss, E., & Hall, J. W., 3rd (2017). Loud music exposure and cochlear synaptopathy in young adults: Isolated auditory brainstem response effects but no perceptual consequences. *Trends in Hearing*, *21*, 2331216517737417.

- Gu, J. W., Halpin, C. F., Nam, E. C., Levine, R. A., & Melcher, J. R. (2010). Tinnitus, diminished sound-level tolerance, and elevated auditory activity in humans with clinically normal hearing sensitivity. *Journal of Neurophysiology*, *104*, 3361–3370.
- Gu, J. W., Herrmann, B. S., Levine, R. A., & Melcher, J. R. (2012). Brainstem auditory evoked potentials suggest a role for the ventral cochlear nucleus in tinnitus. *Journal of the Association for Research in Otolaryngology*, *13*(6), 819–833.
- Guest, H., Munro, K. J., Prendergast, G., Howe, S., & Plack, C. J. (2017). Tinnitus with a normal audiogram: Relation to noise exposure but no evidence for CS. *Hearing Research*, *344*, 265–274.
- Guest, H., Dewey, R. S., Plack, C. J., Couth, S., Prendergast, G., Bakay, W., & Hall, D. A. (2018). The noise exposure structured interview (NESI): An instrument for the comprehensive estimation of lifetime noise exposure. *Trends in hearing*, *22*, 2331216518803213.
- Guest, H., Munro, K. J., Prendergast, G., Millman, R. E., & Plack, C. J. (2018). Impaired speech perception in noise with a normal audiogram: No evidence for cochlear synaptopathy and no relation to lifetime noise exposure. *Hearing Research*, *364*, 142–151.
- Gunderson, E., Moline, J., & Catalano, P. (1997). Risks of developing noise-induced hearing loss in employees of urban music clubs. *American Journal of Industrial Medicine*, *31*(1), 75–79.
- Harrison, R. V., Gordon, K. A., Papsin, B. C., Negandhi, J., & James, A. L. (2015). Auditory neuropathy spectrum disorder (ANSD) and cochlear implantation. *International Journal of Pediatric Otorhinolaryngology*, *79*(12), 1980–1987.

- Henderson, D., Bielefeld, E. C., Lobarinas, E., & Tanaka, C. (2011). Noise-induced hearing loss: implication for tinnitus. In A. R. Møller, B. Langguth, D. DeRidder, & T. Kleinjung (Eds.), *Textbook of tinnitus* (pp. 301–309). New York: Springer.
- Henry, J. A., Dennis, K. C., & Schechter, M. A. (2005). General review of tinnitus: prevalence, mechanisms, effects, and management. *Journal of Speech, Language, and Hearing Research, 48*(5), 1204–1235.
- Henry, J. A., Roberts, L. E., Caspary, D. M., Theodoroff, S. M., & Salvi, R. J. (2014). Underlying mechanisms of tinnitus: Review and clinical implications. *Journal of the American Academy of Audiology, 25*(1), 5–126.
- Hickox, A. E., & Liberman, M. C. (2014). Is noise-induced cochlear neuropathy key to the generation of hyperacusis or tinnitus?. *Journal of Neurophysiology, 111*(3), 552–564.
- Hind, S. E., Haines-Bazrafshan, R., Benton, C. L., Brassington, W., Towle, B., & Moore, D. R. (2011). Prevalence of clinical referrals having hearing thresholds within normal limits. *International Journal of Audiology, 50*(10), 708–716.
- Hunter, L. L., Blankenship, C. M., Gunter, R. G., Keefe, D. H., Feeney, M. P., Brown, D. K., & Baroch, K. (2018). Cochlear microphonic and summing potential responses from click-evoked auditory brain stem responses in high-risk and normal infants. *Journal of the American Academy of Audiology, 29*(5), 427–442.
- Imam, L., & Hannan, S. A. (2017). Noise-induced hearing loss: a modern epidemic?. *British Journal of Hospital Medicine (London, England : 2005), 78*(5), 286–290.
- Johnson, E. D. (1993). Sounds of silence for the walkman generation: Rock concerts and noise-induced hearing loss. *Indiana Law Journal, 68*(3), 22.

- Jokitulppo, J., Toivonen, M., & Björk, E. (2006). Estimated leisure-time noise exposure, hearing thresholds, and hearing symptoms of Finnish conscripts. *Military Medicine*, *171*(2), 112–116.
- Kamerer, A. M., Diaz, F. J., Peppi, M., & Chertoff, M. E. (2016). The potential use of low-frequency tones to locate regions of outer hair cell loss. *Hearing Research*, *342*, 39–47.
- Kardous, C., Themann, C., Morata, T., Reynolds, J., & Afanuh, S. (2015). Reducing the risk of hearing disorders among musicians. *National Institute for Occupational Safety and Health (NIOSH)*, *184*, 1–4.
- Katz, J. (Ed.). (2015). *Handbook of clinical audiology* (7th ed.). Philadelphia, PA: Wolters Kluwer Health.
- Kepler, H., Dhooge, I., & Vinck, B. (2015). Hearing in young adults. Part II: The effects of recreational noise exposure. *Noise & Health*, *17*(78), 245–252.
- Kobel, M., Le Prell, C. G., Liu, J., Hawks, J. W., & Bao, J. (2017). Noise-induced cochlear synaptopathy: Past findings and future studies. *Hearing Research*, *349*, 148–154.
- Kujawa, S. G., & Liberman, M. C. (2006). Acceleration of age-related hearing loss by early noise exposure: Evidence of a misspent youth. *The Journal of Neuroscience*, *26*(7), 2115–2123.
- Kujawa, S. G., & Liberman, M. C. (2009). Adding insult to injury: Cochlear nerve degeneration after “temporary” noise-induced hearing loss. *The Journal of Neuroscience*, *29*(45), 14077–14085.

- Kujawa, S. G., & Liberman, M. C. (2015). Synaptopathy in the noise-exposed and aging cochlea: Primary neural degeneration in acquired sensorineural hearing loss. *Hearing Research, 330*, 191–199.
- Liberman M. C. (2016). Noise-induced hearing loss: Permanent versus temporary threshold shifts and the effects of hair cell versus neuronal degeneration. *Advances in Experimental Medicine and Biology, 875*, 1–7.
- Liberman, M. C., Chesney, C. P., & Kujawa, S. G. (1997). Effects of selective inner hair cell loss on DPOAE and CAP in carboplatin-treated chinchillas. *Auditory Neuroscience, 3*, 255–268.
- Liberman, M. C., Epstein, M. J., Cleveland, S. S., Wang, H., & Maison, S. F. (2016). Toward a Differential Diagnosis of Hidden Hearing Loss in Humans. *PloS one, 11*(9), e0162726.
- Liberman, M. C., & Kiang, N. Y. (1984). Single-neuron labeling and chronic cochlear pathology. IV. Stereocilia damage and alterations in rate- and phase-level functions. *Hearing Research, 16*(1), 75–90.
- Liberman, L. D., & Liberman, M. C. (2019). Cochlear efferent innervation is sparse in humans and decreases with age. *The Journal of Neuroscience, 39*(48), 9560–9569.
- Liberman, M. C., Liberman, L. D., & Maison, S. F. (2015). Chronic conductive hearing loss leads to cochlear degeneration. *PLoS One, 10*(11).
- Lieberman, A., Sohmer, H., & Szabo, G. (1973). Standard values of amplitude and latency of cochlear audiometry (electro-cochleography). Responses in different age groups. *Archiv für Klinische und Experimentelle Ohren- Nasen- und Kehlkopfheilkunde, 203*(4), 267–273.

- Liberman, L. D., Suzuki, J., & Liberman, M. C. (2015). Dynamics of cochlear synaptopathy after acoustic overexposure. *Journal of the Association for Research in Otolaryngology*, *16*(2), 205–219.
- Lichtenhan, J. T., Wilson, U. S., Hancock, K. E., & Guinan, J. J. (2016). Medial olivocochlear efferent reflex inhibition of human cochlear nerve responses. *Hearing Research*, *333*, 216–224.
- Lin, H. W., Furman, A. C., Kujawa, S. G., & Liberman, M. C. (2011). Primary neural degeneration in the Guinea pig cochlea after reversible noise-induced threshold shift. *Journal of the Association for Research in Otolaryngology*, *12*(5), 605–616.
- Lobarinas, E., Salvi, R., & Ding, D. (2013). Insensitivity of the audiogram to carboplatin induced inner hair cell loss in chinchillas. *Hearing Research*, *302*, 113–120.
- Lobarinas, E., Salvi, R., & Ding, D. (2016). Selective inner hair cell dysfunction in chinchillas impairs hearing-in-noise in the absence of outer hair cell loss. *Journal of the Association for Research in Otolaryngology*, *17*(2), 89–101.
- Lüders, D., Gonçalves, C. G., Lacerda, A. B., Silva, L. S., Marques, J. M., & Sperotto, V. N. (2016). Occurrence of tinnitus and other auditory symptoms among musicians playing different instruments. *The International Tinnitus Journal*, *20*(1), 48–53.
- Maison, S. F., Usubuchi, H., & Liberman, M. C. (2013). Efferent feedback minimizes cochlear neuropathy from moderate noise exposure. *The Journal of Neuroscience*, *33*(13), 5542–5552.

- Makary, C. A., Shin, J., Kujawa, S. G., Liberman, M. C., & Merchant, S. N. (2011). Age-related primary cochlear neuronal degeneration in human temporal bones. *Journal of the Association for Research in Otolaryngology*, *12*(6), 711-717.
- Mercier, V., & Hohmann, B. W. (2002). Is electronically amplified music too loud? What do young people think?. *Noise & Health*, *4*(16), 47–55.
- Michalewski, H. J., Starr, A., Nguyen, T. T., Kong, Y. Y., & Zeng, F. G. (2005). Auditory temporal processes in normal-hearing individuals and in patients with auditory neuropathy. *Clinical Neurophysiology*, *116*(3), 669–680.
- Moser, T., & Starr, A. (2016). Auditory neuropathy-neural and synaptic mechanisms. *Neurology*, *12*(3), 135.
- Noguchi, Y., Nishida, H., & Komatsuzaki, A. (1999). A comparison of extratympanic versus transtympanic recordings in electrocochleography. *Audiology*, *38*(3), 135–40.
- Nouvian, R., Beutner, D., Parsons, T., & Moser, T. (2006). Structure and function of the hair cell ribbon synapse. *Journal of Membrane Biology*, *209*, 153–165.
- O'Brien, I., Driscoll, T., & Ackermann, B. (2013). Sound exposure of professional orchestral musicians during solitary practice. *The Journal of the Acoustical Society of America*, *134*(4), 2748–2754.
- Ollick, G. (2016). *A practical approach to clinical electrocochleography (ECoChG)* [White paper]. E3 Diagnostics. <https://www.e3diagnostics.com/-/media/e3-diagnostics/shared/pdf/articles-white-papers/2016/a-practical-approach-to-clinical-electrocochleography-ecochofall-2016.pdf?la=en>.

- Pangrsic, T., Lasarow, L., Reuter, K., Takago, H., Schwander, M., Riedel, D., Frank, T., Tarantino, L. M., Bailey, J. S., Strenzke, N., Brose, N., Müller, U., Reisinger, E., & Moser, T. (2010). Hearing requires otoferlin-dependent efficient replenishment of synaptic vesicles in hair cells. *Nature Neuroscience*, *13*(7), 869–876.
- Parsons, T. D., & Sterling, P. (2003). Synaptic ribbon. Conveyor belt or safety belt?. *Neuron*, *37*(3), 379–382.
- Paul, B. T., Bruce, I. C., & Roberts, L. E. (2017). Evidence that hidden hearing loss underlies amplitude modulation encoding deficits in individuals with and without tinnitus. *Hearing Research*, *344*, 170–182.
- Pawlaczyk-Łuszczynska, M., Dudarewicz, A., Zamojska, M., & Sliwinska-Kowalska, M. (2011). Evaluation of sound exposure and risk of hearing impairment in orchestral musicians. *International Journal of Occupational Safety and Ergonomics*, *17*(3), 255–269.
- Pfeiffer, M., Rocha, R. L. O., Oliveira, F. R., & Frota, S. (2007). Intercorrência audiológica em músicas após um show de rock. *Revista CEFAC*, *9*(3), 423–429.
- Picton, T. W. (2010). Human auditory evoked potentials. Plural Publishing.
- Pienkowski, M. (2017). On the etiology of listening difficulties in noise despite clinically normal audiograms. *Ear and Hearing*, *38*(2), 135–148.
- Plack, C. J., Barker, D., & Prendergast, G. (2014). Perceptual consequences of "hidden" hearing loss. *Trends in Hearing*, *18*, 1–11.

- Plack, C. J., & Oxenham, A. J. (2005). Pitch perception: Neural coding and perception. In C. J. Plack, A. J. Oxenham, A. N. Popper, & R. R. Fay (Eds.), *Pitch: Neural Coding and Perception*. Springer.
- Ponton, C. W., Don, M., & Eggermont, J. J. (1992). Place-specific derived cochlear microphonics from human ears. *Scandinavian Audiology*, *21*(3), 131–141.
- Pouryaghoub, G., Mehrdad, R., & Pourhosein, S. (2017). Noise-Induced hearing loss among professional musicians. *Journal of Occupational Health*, *59*(1), 33–37.
- Pratt, H., Sohmer, H., & Barazani, N. (1978). Surface-recorded cochlear microphonic potentials during temporary threshold shifts in man. *Audiology*, *17*(3), 204–212.
- Prendergast, G., Guest, H., Munro, K. J., Kluk, K., Léger, A., Hall, D. A., Heinz, M. G., & Plack, C. J. (2017). Effects of noise exposure on young adults with normal audiograms I: Electrophysiology. *Hearing Research*, *344*, 68–81.
- Prendergast, G., Millman, R. E., Guest, H., Munro, K. J., Kluk, K., Dewey, R. S., Hall, D. A., Heinz, M. G., & Plack, C. J. (2017). Effects of noise exposure on young adults with normal audiograms II: Behavioral measures. *Hearing Research*, *356*, 74–86.
- Prendergast, G., Tu, W., Guest, H., Millman, R. E., Kluk, K., Couth, S., Munro, K. J., & Plack, C. J. (2018). Supra-threshold auditory brainstem response amplitudes in humans: Test-retest reliability, electrode montage and noise exposure. *Hearing Research*, *364*, 38–47.
- Pujol, R., & Puel, J.-L. (1999). Excitotoxicity, synaptic repair, and functional recovery in the mammalian cochlea: A review of recent findings. *Annals of the New York Academy of Sciences*, *884*, 249254.

- Qian, C. L., Behar, A., & Wong, W. (2011). Noise exposure of musicians of a ballet orchestra. *Noise and Health, 13*(50), 59.
- Rance, G., & Starr, A. (2015). Pathophysiological mechanisms and functional hearing consequences of auditory neuropathy. *Brain, 138*(11), 3141–3158.
- Reddel, R. R., Kefford, R. F., Grant, J. M., Coates, A. S., Fox, R. M., & Tattersall, M. H. (1982). Ototoxicity in patients receiving cisplatin: importance of dose and method of drug administration. *Cancer Treatment Reports, 66*(1), 19–23.
- Riazi, M., & Ferraro, J. A. (2008). Observations on mastoid versus ear canal recorded cochlear microphonic in newborns and adults. *Journal of the American Academy of Audiology, 19*(1), 46–55.
- Roberts, L. E., Moffat, G., Baumann, M., Ward, L. M., & Bosnyak, D. J. (2008). Residual inhibition functions overlap tinnitus spectra and the region of auditory threshold shift. *Journal of the Association for Research in Otolaryngology, 9*(4), 417–435.
- Roberts, L. E., Paul, B. T., & Bruce, I. C. (2018). Erratum and comment: Envelope following responses in normal hearing and in tinnitus. *Hearing Research, 361*, 157–158.
- Roux, I., Safieddine, S., Nouvian, R., Grati, M., Simmler, M. C., Bahloul, A., Perfettini, I., Le Gall, M., Rostaing, P., Hamard, G., Triller, A., Avan, P., Moser, T., & Petit, C. (2006). Otoferlin, defective in a human deafness form, is essential for exocytosis at the auditory ribbon synapse. *Cell, 127*(2), 277–289.
- Ruel, J., Nouvian, R., Gervais d'Aldin, C., Pujol, R., Eybalin, M., & Puel, J. L. (2001). Dopamine inhibition of auditory nerve activity in the adult mammalian cochlea. *The European Journal of Neuroscience, 14*(6), 977–986.

- Ryan, A. F., Kujawa, S. G., Hammill, T., Le Prell, C., & Kil, J. (2016). Temporary and permanent noise-induced threshold shifts: A review of basic and clinical observations. *Otology & Neurotology*, 37(8), e271–e275.
- Rybak, L. P., Mukherjea, D., Jajoo, S., & Ramkumar, V. (2009). Cisplatin ototoxicity and protection: clinical and experimental studies. *The Tohoku Journal of Experimental Medicine*, 219(3), 177–186.
- Salvi, R., Sun, W., Ding, D., Chen, G. D., Lobarinas, E., Wang, J., Radziwon, K., & Auerbach, B. D. (2017). Inner hair cell loss disrupts hearing and cochlear function leading to sensory deprivation and enhanced central auditory gain. *Frontiers in Neuroscience*, 10, 621.
- Santarelli, R., Del Castillo, I., Rodríguez-Ballesteros, M., Scimemi, P., Cama, E., Arslan, E., & Starr, A. (2009). Abnormal cochlear potentials from deaf patients with mutations in the otoferlin gene. *Journal of the Association for Research in Otolaryngology*, 10(4), 545–556.
- Santarelli, R., Scimemi, P., Dal Monte, E., & Arslan, E. (2006). Cochlear microphonic potential recorded by transtympanic electrocochleography in normally-hearing and hearing-impaired ears. *Acta Otorhinolaryngologica Italica*, 26(2), 78–95.
- Sarankumar, T., Arumugam, S. V., Goyal, S., Chauhan, N., Kumari, A., & Kameswaran, M. (2018). Outcomes of cochlear implantation in auditory neuropathy spectrum disorder and the role of cortical auditory evoked potentials in benefit evaluation. *Turkish Archives of Otorhinolaryngology*, 56(1), 15–20.

- Schaette, R., & McAlpine, D. (2011). Tinnitus with a normal audiogram: physiological evidence for hidden hearing loss and computational model. *The Journal of Neuroscience*, *31*(38), 13452–13457.
- Schink, T., Kreutz, G., Busch, V., Pigeot, I., & Ahrens, W. (2014). Incidence and relative risk of hearing disorders in professional musicians. *Occupational and Environmental Medicine*, *71*(7), 472–476
- Schmidt, J. H., Pedersen, E. R., Paarup, H. M., Christensen-Dalsgaard, J., Andersen, T., Poulsen, T., & Bælum, J. (2014). Hearing loss in relation to sound exposure of professional symphony orchestra musicians. *Ear and Hearing*, *35*(4), 448–460.
- Schoonhoven, R., Fabius, M. A., & Grote, J. J. (1995). Input/output curves to tone bursts and clicks in extratympanic and transtympanic electrocochleography. *Ear and Hearing*, *16*(6), 619–630.
- Sergeyenko, Y., Lall, K., Liberman, M. C., & Kujawa, S. G. (2013). Age-related cochlear synaptopathy: An early-onset contributor to auditory functional decline. *The Journal of Neuroscience*, *33*(34), 13686–13694.
- Shaheen, L. A., Valero, M. D., & Liberman, M. C. (2015). Towards a diagnosis of cochlear neuropathy with envelope following responses. *Journal of the Association for Research in Otolaryngology*, *16*(6), 727–745.
- Shaikh, A. M. A., Eldin, H. E., & Abusetta, A. (2016). Outcome of auditory neuropathy spectrum disorder after cochlear implantation. *Journal of Child Development Disorders*, *2*(3), 19.
- Shargorodsky, J., Curhan, G. C., & Farwell, W. R. (2010). Prevalence and characteristics of tinnitus among US adults. *The American Journal of Medicine*, *123*(8), 711–718.

- Shi, W., Ji, F., Lan, L., Liang, S., Ding, H., Wang, H., & Wang, Q. (2012). Characteristics of cochlear microphonics in infants and young children with auditory neuropathy. *Acta Oto-Laryngologica, 132*(2), 188-196.
- Simpson, M. J., Jennings, S. G., & Margolis, R. H. (2020). Techniques for obtaining high-quality recordings in electrocochleography. *Frontiers in Systems Neuroscience, 14*, 18.
- Sliwinska-Kowalska, M., & Davis, A. (2012). Noise-induced hearing loss. *Noise & Health, 14*(61), 274–280.
- Smith, K. (2018). Cochlear microphonics from auditory brainstem responses of infants with auditory neuropathy spectrum disorder. *The University of British Columbia*. Retrieved from <http://hdl.handle.net/2429/67184>.
- Soares, I. D., Menezes, P. L., Carnaúba, A. T., de Andrade, K. C., & Lins, O. G. (2016). Study of cochlear microphonic potentials in auditory neuropathy. *Brazilian Journal of Otorhinolaryngology, 82*(6), 722–736.
- Sohmer, H., & Feinmesser, M. (1967). Cochlear action potentials recorded from the external ear in man. *Annals of Otology, Rhinology & Laryngology, 76*(2), 427–35.
- Sohmer, H., & Pratt, H. (1976). Recording of the cochlear microphonic potential with surface electrodes. *Electroencephalography and Clinical Neurophysiology, 40*(3), 253–260.
- Song, Q., Shen, P., Li, X., Shi, L., Liu, L., Wang, J., Yu, Z., Stephen, K., Aiken, S., Yin, S., & Wang, J. (2016). Coding deficits in hidden hearing loss induced by noise: The nature and impacts. *Scientific Reports, 6*, 25200.

- Spencer, R. F., Shaia, W. T., Gleason, A. T., Sismanis, A., & Shapiro, S. M. (2002). Changes in calcium-binding protein expression in the auditory brainstem nuclei of the jaundiced Gunn rat. *Hearing Research, 171*(1-2), 129–141.
- Stamper, G. C., & Johnson, T. A. (2015). Auditory function in normal-hearing, noise-exposed human ears. *Ear and Hearing, 36*(2), 172–184.
- Stamper, G.C., & Johnson, T.A. (2015). Letter to the editor: Examination of potential sex influences in Auditory function in normal-hearing, noise-exposed human ears, *Ear Hear, 36*, 172-184. *Ear and Hearing, 36*(2), 738–740.
- Starr, A., Picton, T. W., Sininger, Y., Hood, L. J., & Berlin, C. I. (1996). Auditory neuropathy. *Brain, 119*(3), 741–753.
- Starr, A., Sininger, Y., Nguyen, T., Michalewski, H. J., Oba, S., & Abdala, C. (2001). Cochlear receptor (microphonic and summing potentials, otoacoustic emissions) and auditory pathway (auditory brain stem potentials) activity in auditory neuropathy. *Ear and Hearing, 22*(2), 91–99.
- Teagle, H. F., Roush, P. A., Woodard, J. S., Hatch, D. R., Zdanski, C. J., Buss, E., & Buchman, C. A. (2010). Cochlear implantation in children with auditory neuropathy spectrum disorder. *Ear and Hearing, 31*(3), 325–335.
- Tremblay, K. L., Pinto, A., Fischer, M. E., Klein, B. E., Klein, R., Levy, S., Tweed, T. S., & Cruickshanks, K. J. (2015). Self-reported hearing difficulties among adults with normal audiograms: The beaver dam offspring study. *Ear and hearing, 36*(6), 290–299.

- Valderrama, J. T., Beach, E. F., Yeend, I., Sharma, M., Van Dun, B., & Dillon, H. (2018). Effects of lifetime noise exposure on the middle-age human auditory brainstem response, tinnitus and speech-in-noise intelligibility. *Hearing Research*, 365, 36–48.
- Valero, M. D., Hancock, K. E., & Liberman, M. C. (2016). The middle ear muscle reflex in the diagnosis of cochlear neuropathy. *Hearing Research*, 332, 29–38.
- Valero, M. D., Hancock, K. E., Maison, S. F., & Liberman, M. C. (2018). Effects of cochlear synaptopathy on middle-ear muscle reflexes in unanesthetized mice. *Hearing Research*, 363, 109–118.
- Viana, L. M., O'Malley, J. T., Burgess, B. J., Jones, D. D., Oliveira, C. A., Santos, F., ... & Liberman, M. C. (2015). Cochlear neuropathy in human presbycusis: Confocal analysis of hidden hearing loss in post-mortem tissue. *Hearing Research*, 327, 78–88.
- Vlastarakos, P. V., Nikolopoulos, T. P., Tavoulari, E., Papacharalambous, G., & Korres, S. (2008). Auditory neuropathy: Endocochlear lesion or temporal processing impairment? Implications for diagnosis and management. *International Journal of Pediatric Otorhinolaryngology*, 72(8), 1135–1150.
- Wang, Y., Hirose, K., & Liberman, M. C. (2002). Dynamics of noise-induced cellular injury and repair in the mouse cochlea. *Journal of the Association for Research in Otolaryngology : JARO*, 3(3), 248–268.
- Washnik, N. J., Bhatt, I. S., Phillips, S. L., Tucker, D., & Richter, S. (2020). Evaluation of cochlear activity in normal-hearing musicians. *Hearing Research*, 395, 108027.

- Wojtczak, M., Beim, J. A., & Oxenham, A. J. (2017). Weak middle-ear-muscle reflex in humans with noise-induced tinnitus and normal hearing may reflect cochlear synaptopathy. *eNeuro*, 4(6), ENEURO.0363-17.2017.
- Yassi, A., Pollock, N., Tran, N., & Cheang, M. (1993). Risks to hearing from a rock concert. *Canadian Family Physician Medecin de Famille Canadien*, 39, 1045–1050.
- Yoshie, N., & Yamaura, K. (1969). Cochlear microphonic responses to pure tones in man recorded by a non-surgical method. *Acta Oto-Laryngologica*, 252, 37–69.
- Young, E. D., & Barta, P. E. (1986). Rate responses of auditory nerve fibers to tones in noise near masked threshold. *The Journal of the Acoustical Society of America*, 79(2), 426–442.
- Zeng, F. G., Kong, Y. Y., Michalewski, H. J., & Starr, A. (2005). Perceptual consequences of disrupted auditory nerve activity. *Journal of Neurophysiology*, 93(6), 3050–3063.
- Zhang, M. (2012). Response pattern based on the amplitude of ear canal recorded cochlear microphonic waveforms across acoustic frequencies in normal hearing subjects. *Trends in Amplification*, 16(2), 117–126.

Appendices

Appendix A Supporting Documents

A.1 Pearson's r Correlations

Inter-Rater Pearson Correlations (r (41))			
CM Measure	Rater 1 vs Rater 2	Rater 1 vs Rater 3	Rater 2 vs Rater 3
CM Duration (lib)	0.498 (p = 0.001)	0.024 (p = 0.444)	0.141 (p = 0.199)
CM Duration (con)	0.299 (p = 0.034)	0.220 (p = 0.092)	0.157 (p = 0.173)
CM/CAP Amplitude (lib)	0.991 (p = 0.000)	0.980 (p = 0.000)	0.976 (p = 0.000)
CM/CAP Amplitude (con)	0.986 (p = 0.000)	0.991 (p = 0.000)	0.981 (p = 0.000)
CM Power (lib)	0.966 (p = 0.000)	0.951 (p = 0.000)	0.937 (p = 0.000)
CM Power (con)	0.926 (p = 0.000)	0.953 (p = 0.000)	0.917 (p = 0.000)

A.2 CM ANSD Literature

Study	Recording Method	Groups	Subject Age	CM Data
Smith (2018)	ABR	1) ANSD 2) & 3) Hunter et al. (2018) groups	Mean: 3.5 ± 3.2 months	<p><i>Duration:</i> ANSD = 4.197 ± 1.154 ms OAE+ = 3.971 ± 1.108 ms OAE- = 4.746 ± 1.157 ms</p> <p><i>Amplitude:</i> ANSD = 0.322 ± 0.173 μV</p> <p><i>Amplitude Ratio (CM/V):</i> OAE+ = 6.602 ± 2.987 μV OAE- = 2.040 ± 1.112 μV</p>
Hunter (2018)	ABR	1) High-risk neonatal intensive care babies 2) Healthy controls	Mean: 1.25 months	<p><i>Duration:</i> Control = 0.73 ± 0.3ms NICU = 0.82 ± 0.51ms ANSD case at: - 3 months = 1.82ms (left), 1.49ms (right) - 8 months = 1.22ms (left), 0.99ms (right)</p> <p><i>Amplitude:</i> Control = 0.24 ± 0.09 μV NICU = $0.26 \pm 0.13$$\mu$V ANSD case at: - 3 months (70 db nHL) = 0.20 μV (left), 0.14 μV (right) - 8 months (80 dB nHL) = 0.4μV (left) and 0.5 μV (right)</p>
CONTINUED...				

Study	Recording Method	Groups	Subject Age	CM Data
Santarelli et al. (2006)	TT and ET ECoChG	1) ANSD 2) Central nervous system disorder present 3) Controls	Mean: 3.1 ± 3.9 years Range: 7 months to 47 years	<p><i>Duration:</i> ANSD = 6.77 ± 2.58ms CNS+ = 7.99 ± 2.49ms Control = 4.36 ± 1.97ms</p> <p><i>Amplitude (120 dB peSPL):</i> ANSD = 13.5 ± 26.8µV CNS+ = 32.2 ± 36.6 µV Control = 18.8 ± 12.8 µV</p>
Starr et al. (2001)	ABR	1) ANSD 2) Controls	Range: 0.25 months to 64 years	<p><i>Duration:</i> Control = could not evaluate after 0.7ms ANSD = persisted for several milliseconds after a transient stimulus</p> <p><i>Amplitude:</i> (Mean value listed in paper): ANSD (TEOAEs present) = 0.42 ± 0.29µV. (Approximate values from Figure 2 in paper): Controls = 0.1-0.5 µV ANSD = 0.1-1.3 µV</p>

Appendix B Descriptive Statistics

B.1 CM Duration

CM Duration				
Liberal			Conservative	
Rater 1	High-risk	Control	High-risk	Control
Median	3.4000	3.0850	2.8000	2.6150
Mean	3.4474	3.2193	2.7589	2.7936
SD	0.9341	0.7352	0.8809	0.7541
Minimum	1.7700	2.2000	0.9700	1.7000
Maximum	5.3300	4.5300	4.8300	4.4700
Rater 2	High-risk	Control	High-risk	Control
Median	3.170	2.765	1.600	1.200
Mean	3.250	2.926	1.755	1.555
SD	1.306	1.247	0.916	0.874
Minimum	0.700	0.730	0.670	0.670
Maximum	6.200	4.800	4.130	2.970
Rater 3	High-risk	Control	High-risk	Control
Median	4.8700	4.6500	2.6300	2.6300
Mean	4.7378	4.8171	2.7496	2.5221
SD	1.2478	1.1137	1.0040	0.6345
Minimum	2.0300	3.2300	0.8000	1.5000
Maximum	7.7300	6.4700	4.8700	3.5700

B.2 CM/CAP Amplitude Ratio

CM/CAP Amplitude Ratio				
Liberal			Conservative	
Rater 1	High-risk	Control	High-risk	Control
Median	1.0348	0.9963	1.0235	0.9963
Mean	1.9414	1.0226	1.9300	1.0770
SD	1.9244	0.7535	1.9310	0.7066
Minimum	0.2307	0.0839	0.2307	0.1532
Maximum	7.7117	3.0755	7.7117	3.0755
Rater 2	High-risk	Control	High-risk	Control
Median	1.060	0.825	0.890	0.675
Mean	1.876	0.992	1.801	0.859
SD	1.758	0.657	1.809	0.683
Minimum	0.450	0.160	0.240	0.160
Maximum	6.670	2.780	6.670	2.780
Rater 3	High-risk	Control	High-risk	Control
Median	1.0164	0.8965	1.1475	0.8745
Mean	1.7825	0.9634	1.8725	0.9837
SD	1.8854	0.5597	1.8208	0.5949
Minimum	0.3908	0.3799	0.3878	0.3025
Maximum	7.7117	2.5888	7.7117	2.5888

B.3 CM Power

CM Power				
Liberal			Conservative	
Rater 1	High-risk	Control	High-risk	Control
Median	0.00070	0.00075	0.00070	0.00070
Mean	0.00094	0.00101	0.00085	0.00090
SD	0.00075	0.00066	0.00072	0.00055
Minimum	0.00010	0.00040	0.00010	0.00030
Maximum	0.00360	0.00230	0.00340	0.00210
Rater 2	High-risk	Control	High-risk	Control
Median	0.00070	0.00070	0.00020	0.00060
Mean	0.00086	0.00093	0.00051	0.00078
SD	0.00071	0.00075	0.00062	0.00061
Minimum	0.00000	0.00020	0.00000	0.00020
Maximum	0.00310	0.00250	0.00270	0.00200
Rater 3	High-risk	Control	High-risk	Control
Median	0.00090	0.00090	0.00070	0.00065
Mean	0.00112	0.00109	0.00080	0.00084
SD	0.00068	0.00057	0.00054	0.00054
Minimum	0.00020	0.00040	0.00010	0.00030
Maximum	0.00340	0.00220	0.00260	0.00200